TRIPLET PRODUCTION BY A POLARIZED PHOTON BEAM ON A POLARIZED ELECTRON TARGET

G.I. Gakh[1,2], M.I. Konchatnij[1], N.P. Merenkov[1,2]
[1]NSC "Kharkov Institute of Physics and Technology"
Akademicheskaya, 1, 61108 Kharkov, Ukraine
[2]V.N. Karazin Kharkiv National University, 61022 Kharkov, Ukraine
e-mail: konchatnij@kipt.kharkov.ua
Received December 14, 2015

The cross section and polarization observables in the process of the electron-positron pair photoproduction on a free electron are calculated. The double differential distributions, over the square of the 4-momentum transfer to the recoil electron q^2, and the square of the created e^+e^- - invariant mass, Q^2 are obtained in the target-electron rest frame taking into account the contributions of the so-called Borsellino and $(\gamma - e)$ diagrams. The integration of these distributions over q^2 (and over Q^2) is performed and the results are analyzed mainly in those kinematical regions where the $(\gamma - e)$ -contribution is larger (or the same order) than (as) the Borsellino one. Such calculations are motivated by the experiments in search of the possible dark matter candidate (light U-boson) in process of triplet photoproduction. The original analytical formulas for q^2 (and Q^2) distributions can be used to check the work of the corresponding Monte Carlo generators. We consider the following cases: particles are unpolarized, photon beam is linearly polarized, photon beam is circularly polarized at polarized electron target.
KEY WORDS: triplet, polarization, cross section, the Stokes parameters, photon beam

НАРОДЖЕННЯ ТРИПЛЕТА ПОЛЯРИЗОВАНИМ ФОТОННИМ ПУЧКОМ НА ПОЛЯРИЗОВАНІЙ ЕЛЕКТРОННІЙ МІШЕНІ
Г.И. Гах[1,2], М.И. Кончатний[1], М.П. Меренков[1,2]
[1] *Національний науковий центр «Харківський фізико-технічний інститут»*
61108 Україна, м. Харків, вул. Академічна, 1
[2] *Харківський національний університет імені В.Н. Каразіна*
61022, Україна, м. Харків, пл. Свободи, 4

Обчислені переріз та поляризаційні спостережувані в процесі фотонародження електронно-позитронних пар на вільних електронах. З врахуванням вкладів так званних Борселіно- та $(\gamma - e)$ -діаграм отримані двічі диференцфійні розподіли по квадрату 4-імпульсу q^2, переданого електрону віддачі, та квадрату інваріантної маси Q^2 народженної e^+e^- -пари в системі спокою електрона-мішені. Виконано інтегрування цих расподілів по q^2 (або по Q^2) і результати проаналізовані в основному в тих кінематичних областях, де $(\gamma - e)$ -вклад більше (або одного порядку) вкладу (з вкладом) Борселіно. Такі розрахунки мотивовані експериментами по пошуку одного з претендентів на темну матерію – легкого U-бозону – в процесі фотонародження триплетів. Оригінальні аналітичні формулі для q^2 (і Q^2) разподілів можуть бути використані для перевірки роботи відповідних Монте Карло генераторів. Нами розглянуті наступні випадки: частинки не поляризовані, фотонний пучок поляризований лінійно, фотонний пучок поляризований циркулярно при поляризованій електронній мішені.
КЛЮЧОВІ СЛОВА: триплет, поляризація, переріз, параметри Стокса, фотонний пучок.

РОЖДЕНИЕ ТРИПЛЕТА ПОЛЯРИЗОВАННЫМ ФОТОННЫМ ПУЧКОМ НА ПОЛЯРИЗОВАННОЙ ЭЛЕКТРОННОЙ МИШЕНИ
Г.И. Гах[1,2], М.И. Кончатный[1], Н.П. Меренков[1,2]
[1] *Национальный научный центр «Харьковский физико-технический институт»*
61108, Украина, г. Харьков, ул. Академическая, 1
[2] *Харьковский национальный университет им. В.Н. Каразина*
61022, Украина, г. Харьков, пл. Свободы, 4

Вычислены сечение и поляризационные наблюдаемые в процессе фоторождения электронно-позитронных пар на свободных электронах. С учётом вкладов так называемых Борселино- и $(\gamma - e)$ -диаграмм получены дважды дифференциальные распределения по квадрату 4-импульса q^2, переданного электрону отдачи, и квадрату инвариантной массы Q^2 образованной e^+e^- -пары в системе покоя электрона-мишени. Выполнено интегрирование этих распределений по q^2 (или по Q^2) и результаты проанализированы в основном в тех кинематических областях, где $(\gamma - e)$ -вклад больше (или одного порядка) вклада (с вкладом) Борселино. Такие расчёты мотивированы экспериментами по поиску одного из претендентов на темную материю – легкого U-бозона – в процессе фоторождения триплетов. Оригинальные аналитические

формулы для q^2 (и Q^2) распределений могут быть использованы для проверки работы соответствующих Монте Карло генераторов. Нами рассмотрены следующие случаи: частицы не поляризованы, фотонный пучок поляризован линейно, фотонный пучок поляризован циркулярно при поляризованной электронной мишени.

КЛЮЧЕВЫЕ СЛОВА: триплет, поляризация, сечение, пораметры Стокса, фотонный пучок

Many authors have studied theoretically the process of the triplet photoproduction (TPP) by an unpolarized photon on free electrons. This process is completely described by 8 Feynman diagrams. Therefore, the exact expressions for the differential and partly integrated cross sections of the TPP process are very cumbersome and exist in the complete form only in the unpolarized case [1]. That is why, the usual practice, in the calculations of various observables, was to use approximations: for example, to consider the high-energy limit or to neglect some of the Feynman diagrams. The approximation, when only the so-called Borsellino diagrams (Fig. 1a) are taken into account, is the most often used in the calculations.
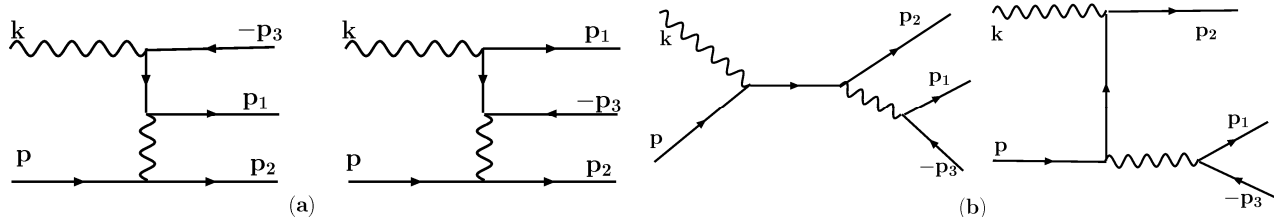

Fig.1. Feynman diagrams describing the process of the triplet photoproduction on free electrons (the exchange diagrams are omitted). The diagrams (a) are the Borsellino's ones, and the diagrams (b) are the $\gamma - e$ ones.

Borsellino [2] calculated the cross section of the TPP process by neglecting the exchange and $\gamma - e$ diagrams (Fig. 1b). He derived formula for the total cross section in the high-energy limit. Mork [3] calculated numerically the total cross section of the TPP reaction. He calculated separately the contributions to the total cross section from the full set of the Feynman diagrams (Borsellino, $\gamma - e$ and exchange terms). It was found that the Borsellino's calculation [2] for the total cross section is valid for $E_\gamma \geq 8$ MeV. The calculated recoil-electron momentum distribution is also agrees with the Borsellino result which is valid if the exchange and $\gamma - e$ terms can be neglected. Mork showed that the Borsellino's distribution is valid for $E_\gamma \geq 8$ MeV if the energy of the recoil electron is well below the energy of the electron produced. Because Mork took into account all diagrams, he has verified the accuracy and limitations of the previous calculations. Haug [1] took into account all diagrams and calculated analytically the angular distribution and energy spectra of the produced positron as well as the total cross section. Later [4], the total cross section is fitted to simple analytic expressions in four intervals of the incident photon energy which cover the entire range between threshold and infinity. Endo and Kobayashi [5] calculated numerically the differential cross section of the TPP on an electron target in the photon energy region $E_\gamma = 50 - 550$ MeV. They took into account all eight Feynman diagrams, i.e., the calculation was done without any approximation. For the recoil-electron momentum distribution, it turned out that the calculation with only the Borsellino diagrams agrees very well with the full calculation. The total cross sections for the process of n electron-positron pair production in photon-electron collisions have been calculated at high energy in the main logarithmic approximation [6]. In the work [7], the authors have analyzed 8 Feynman diagrams and have shown that for energies lower to ~ 500 MeV, the assumption about clear distinction between recoil and created electrons is not a good approximation. They proposed the way to solve this problem.

The authors of Ref. [8] obtained the expression for the Compton tensor of the fourth rank, which determines the Borsellino diagrams, in the case when the integration over the produced electron-positron pair variables has been performed using the method of the invariant integration. This calculation was done for the general case of two virtual photons.

A few papers were devoted to the investigation of the polarization effects in the triplet photoproduction on an electron. The authors of the paper [9] calculated the differential cross section in the azimuthal angle of the recoil electrons in the case of the linearly polarized photons taking into account the Borsellino diagrams only. The cross section asymmetry slowly decreases from 30% at the 10 MeV of the photon beam energy down to 14% in the far asymptotic. Later, they [10] investigated the influence on the asymmetry of the minimal detected recoil momentum. The possibility of the determination of the degree of a linearly polarized photon beam with the help of the triplet photoproduction was studied also in Refs. [11,12]. The differential cross section with respect to the azimuthal angle is determined [11] for extremely high photon energies in laboratory system. The distribution with respect to the polar angle of the recoil electrons is discussed also in this paper. The authors of Ref. [12] calculated the recoil electron distribution and the energy distribution of one of the pair components as well as the positron (electron) spectrum in the case when the recoil momentum is being fixed. The authors of Ref. [5] calculated the cross section as a function of azimuthal angle of the recoil electron and obtained the analyzing power for the polarimetry of linearly polarized photons. It was found that the analyzing power is greatly enhanced by selecting the events with small opening angles

between the forward going electron and positron. The detailed description of the various differential distributions, such as the dependence on the momentum value, on the polar angle and minimal recorded momentum of the recoil electron, dependence on the invariant mass of the created electron-positron pair, on the positron energy and others, has been investigated in Ref. [13]. The authors of Ref. [14] calculated the power corrections of the order of m/ω (m is the electron mass and ω is the energy of the photon beam in the laboratory system), but only due to the interferences of the Borsellino diagrams with all the rest ones, to the distribution of the recoil-electron momentum and azimuthal angle. They estimated the deviation from the asymptotic result [11] for various values of ω. The possibility of the determining the circular polarization of a high-energy photon beam by the measuring the created electron polarization was investigated in Ref. [15], taking into account the contribution of the Borsellino diagrams. Different double and single distributions of the created electron were calculated.

Note that the polarization effects in the TPP process were calculated, up to now, in the approximation when only the Borsellinos' diagrams were taken into account. Such approximation was checked by many authors for the calculated unpolarized observables such as the total cross section, the distribution over the recoil-electron variables. It was found that such approximation is valid for the photon-beam energies $\geq$ 10 MeV. But such verification was not performed for the investigated polarization observables in the TPP process. That is why, in this paper, we calculated the polarization observables taking into account not only the Borsellinos' diagrams but we take also into account the $\gamma - e$ diagrams.

The results of the paper [9] stimulated a search for the construction of a good polarimetry for high-energy photons above an energy of a few hundred MeV. So, for the measurement of the photon-beam linear polarization it was worthwhile to develop polarimetry on the basis of the detection of the recoil electrons from the TPP process. For example, the authors of Ref. [16] constructed a scintillation counting system for detecting the recoils electrons in TPP process. It was tested by using tagged photons with $E_\gamma = 120 \div 400$ MeV and probed to be capable of identifying the TPP events with recoil-electron momenta 1.92 - 10 MeV/c.

The astrophysics community shows interest in measuring the polarization of the cosmic gamma rays of the high energy: for example, the proposal Hard X and Gamma-ray Polarization (see references in [17]). The problem of the measurement of the $\gamma\gamma$ and γe luminosities and polarizations at photon colliders has been considered in Ref. [18]. There are two QED processes are of interest to measure the γe luminosity: the Compton scattering $\gamma + e \rightarrow \gamma + e$ and the TPP reaction on free electron $\gamma + e \rightarrow e + e + e$. At small angles the TPP cross section is even larger and this cross section only weakly depends on the polarization of the initial particles. The study of the TPP process on a free electron is a part of the proposed physics program at the planned high luminosity linac IRIDE (Interdisciplinary Research Infrastructure based on Dual Electron linac and laser), Frascati [19]. At IRIDE one can search for a new, beyond Standard Model, weakly interacting U boson (see, for example, [20]). Its existence can explain several puzzling astrophysical observations (PAMELA abundance of positrons and others). The mass of the U boson is expected to be at MeV or GeV scale. Thus, the QED triplet production is the main background in the search of U boson in the electron-photon scattering that requires the precise measurement of the triplet production. This, in its turn, needs the precise theoretical calculations for the various observables in the TPP process.

In this paper we calculate polarized and unpolarized observables in the TPP process on a free electron in the approximation when the Borsellino and $\gamma - e$ diagrams are taken into account. Integrating the differential cross section over the produced electron-positron pair variables, using the method of the invariant integration, we obtain the analytical form of the distribution over the recoil-electron variables. These are the squared invariant mass of the created e^+e^- pair $(p_1 + p_3)^2$, and squared momentum transferred $(p_2 - p)^2$. For the definition of the particle 4-momenta see Fig. 1. Really, our results describe the events with well separated created and recoil electrons. Otherwise, the effects due to the identity of the final electrons have to be taken into account. In this case, the investigation of double distributions over both $(p_1 + p_3)^2$ and $(p_2 + p_3)^2$ variables seems more natural. We believe that search for U-boson at IRIDE can be performed in the kinematical regions where the contribution of the $\gamma - e$ diagrams is at least of the same order as the Borsellino ones. Besides, we understand that at this condition the identity effects have become essential. Thus, for the U-boson search our results have to be recalculated. Nevertheless, they can be used to determine the optimal kinematical region and to test the Monte Carlo generators which used for analysis of the real experiments. In what follows we consider the following cases: unpolarized particles, the photon beam is linear polarized and circularly polarized photon beam interacts with a polarized electron target. The influence of the $\gamma - e$ terms on the azimuthal asymmetry, due to the linearly polarized beam, and on the double-spin asymmetry, caused by the circularly polarized photon beam and electron-target polarization, has been investigated. The analytical expressions are obtained for various observables and the numerical estimations of the polarization effects have been done. Most of our analytical results are absent in the literature.

The goal of the paper is to investigate the differential cross section and polarisation observables fot the triplet photoproduction process in the kinematical region where the contribution $\gamma - e$ mechanism is the same order as of the contribution of the Borsellino diagrams.

In Section "MATRIX ELEMENT AND CROSS SECTION" the matrix element describing the Borsellino and

$\gamma - e$ diagrams is given. In Section "THE BORSELLINO CONTRIBUTION" the tensors defining the Borsellino diagrams were calculated and the distributions over the q^2, Q^2 and ϕ (the azimuthal angle of the recoil electron) variables were obtained for the following conditions: all particles are unpolarized, the photon beam is linearly polarized and circularly polarized photon beam interacts with a polarized electron target. In Section "THE $\gamma - e$ CONTRIBUTION" the similar calculations were done for the $\gamma - e$ diagrams. Section "DIFFERENT DISTRIBUTIONS" contains the results of calculation of the double (over the q^2 and Q^2 variables) and single (over the q^2 or Q^2 variable) distributions for the same polarization situations. The results and discussion are presented in one Section "RESULTS AND DISCUSSION". Finally, in last Section we give some conclusions.

MATRIX ELEMENT AND CROSS SECTION

The reaction of the triplet production by a photon beam on an electron target

$$\gamma(k) + e^-(p) \rightarrow e^-(p_1) + e^+(p_3) + e^-(p_2), \tag{1}$$

where 4-momenta of the particles are shown in the parentheses, is described, in general, by eight Feynman diagrams. In the calculations we take into account four Feynman diagrams: the so-called Borsellino diagrams (see Fig. 1a) and the $\gamma - e$ ones (see Fig. 1b), i.e., we neglect the effects of the identity of the final electrons.

Therefore, in this approximation, the matrix element of the reaction (1) can be written as follows

$$M = M(B) + M(C), \tag{2}$$

where $M(B)(M(C))$ is the contribution of two Borsellino (($\gamma - e$) or Compton-like) diagrams. These contributions have the following form

$$M(B) = (4\pi\alpha)^{\frac{3}{2}} q^{-2} A_\mu j_\mu(B), \quad M(C) = (4\pi\alpha)^{\frac{3}{2}} Q^{-2} A_\mu j_\mu(C), \tag{3}$$

where $q = p - p_2, Q = p_1 + p_3, \alpha = e^2 / 4\pi = 1/137$, A_μ is the polarization 4-vector of the initial photon.

The currents corresponding to the Borsellino and the $\gamma - e$ diagrams can be written as

$$j_\mu(B) = \bar{u}(p_2)\gamma_\lambda u(p) \bar{u}(p_1)\hat{Q}_{\mu\lambda} u(-p_3), \quad \hat{Q}_{\mu\lambda} = \frac{1}{2d_1}\gamma_\mu \hat{k} \gamma_\lambda - \frac{1}{2d_3}\gamma_\lambda \hat{k} \gamma_\mu + e_\mu^{(31)}\gamma_\lambda, \tag{4}$$

$$j_\mu(C) = \bar{u}(p_1)\gamma_\lambda u(-p_3)\bar{u}(p_2)\hat{K}_{\mu\lambda} u(p), \quad \hat{K}_{\mu\lambda} = \frac{1}{2d_2}\gamma_\mu \hat{k} \gamma_\lambda + \frac{1}{2d}\gamma_\lambda \hat{k} \gamma_\mu - e_\mu^{(20)}\gamma_\lambda,$$

where we introduce the following notation

$$e_\mu^{(20)} = \frac{p_{2\mu}}{d_2} - \frac{p_\mu}{d}, \quad e_\mu^{(31)} = \frac{p_{3\mu}}{d_3} - \frac{p_{1\mu}}{d_1},$$

$d = (kp), d_i = (kp_i)$ (i=1,2,3).

In the case when the polarization state of the photon beam is described by the spin-density matrix, the square of the matrix element can be written as follows

$$|M|^2 = (4\pi\alpha)^3 \rho_{\mu\nu}^\gamma [q^{-4}T_{\mu\nu}(B) + Q^{-4}T_{\mu\nu}(C) + q^{-2}Q^{-2}T_{\mu\nu}(BC)], \tag{5}$$

where $\rho_{\mu\nu}^\gamma$ is the photon-beam spin-density matrix and we use the following covariant expression for it

$$\rho_{\mu\nu}^\gamma = \frac{1}{2}([e_{1\mu}e_{1\nu} + e_{2\mu}e_{2\nu}] + \xi_3[e_{1\mu}e_{1\nu} - e_{2\mu}e_{2\nu}] + \xi_1[e_{1\mu}e_{2\nu} + e_{2\mu}e_{1\nu}] - i\xi_2[e_{1\mu}e_{2\nu} - e_{2\mu}e_{1\nu}]), \tag{6}$$

where ξ_i are the Stokes parameters and the mutually orthogonal space-like 4-vectors e_1 and e_2, relative to which the

photon polarization properties are defined, have to satisfy the following relations

$$e_1^2 = e_2^2 = -1, \quad (e_1 k) = (e_2 k) = (e_1 e_2) = 0. \tag{7}$$

The first term inside the parentheses in r.h.s. of Eq. (6) corresponds to the events with unpolarized photon, the second and third ones are responsible for the events with linear photon polarization and the last one – for the events with the circular polarization. The Stokes parameters ξ_1 and ξ_3, which define the linear polarization degree of the photon, depend on the choice of the 4-vectors e_1 and e_2, whereas the parameter ξ_2 does not depend. As the 4-vectors e_i we choose the following:

$$e_1 = (0, \vec{e}_1), \ e_2 = (0, \vec{e}_2), \ \vec{e}_1{}^2 = \vec{e}_2{}^2 = 1, \ (\vec{e}_1 \vec{e}_2) = 0. \tag{8}$$

In the laboratory system, we define a coordinate system with the z axis directed along the photon-beam momentum $\vec{k}$, and the $x(y)$ axis directed along the vector $\vec{e}_1(\vec{e}_2)$. In this case, the recoil-electron momentum $\vec{p}_2$ is determined by the polar and azimuthal angles θ and ϕ, respectively (Fig. 2).
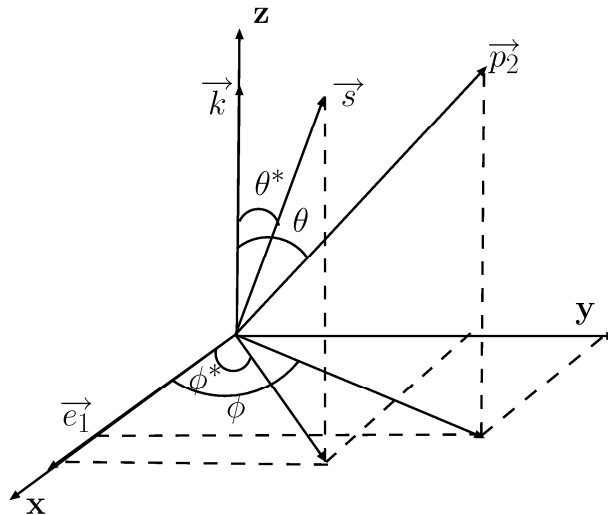

Fig. 2. The angles defining the kinematics of the triplet photoproduction process in the laboratory system. $\vec{e}_1$ is the photon-beam polarization vector, $\vec{s}$ is the electron polarization vector, $\vec{k}(\vec{p}_2)$ is the photon-beam (recoil-electron) momentum.

If we define two orthogonal space-like unit four-vectors

$$A_{1\mu} = \frac{dp_{2\mu} - d_2 p_\mu}{N}, \quad A_{2\mu} = \frac{<\mu k p p_2>}{N}, \quad N^2 = 2d\,d_2(pp_2) - m^2(d^2 + d_2^2),$$

for the description of the photon polarization states, then up to the gauge transformation we can write

$$e_{1\mu} = A_{1\mu} \cos\phi - A_{2\mu} \sin\phi, \quad e_{2\mu} = A_{1\mu} \sin\phi + A_{2\mu} \cos\phi,$$

where $<\mu k p p_2> = \varepsilon_{\mu\alpha\beta\gamma} k_\alpha p_\beta p_{2\gamma}, \quad \varepsilon_{1234} = 1$.

The tensors $T_{\mu\nu}(B)(T_{\mu\nu}(C))$ and $T_{\mu\nu}(BC)$ correspond to the contribution of the Borsellino ($\gamma - e$) diagrams and to the interference between the Borsellino and $\gamma - e$ diagrams. They are defined as follows

$$T_{\mu\nu}(B) = j_\mu(B) j_\nu^*(B), \quad T_{\mu\nu}(C) = j_\mu(C) j_\nu^*(C), \quad T_{\mu\nu}(BC) = j_\mu(B) j_\nu^*(C) + j_\mu(C) j_\nu^*(B). \tag{9}$$

The differential cross section can be written in the form

$$d\sigma = \frac{(2\pi)^{-5}}{32I} |M|^2 \frac{d^3 p_1}{E_1} \frac{d^3 p_2}{E_2} \frac{d^3 p_3}{E_3} \delta^{(4)}(k + p - p_1 - p_2 - p_3), \tag{10}$$

where $I = (kp)$. The factors, which correspond to the averaging over the spins of the photon beam and initial electron, are included in $|M|^2$.

Consider the experimental setup when the produced electron-positron pair is not detected. In this case, it is necessary to integrate over the variables of this pair. The most convenient way to do this is to use the method of the invariant integration. In this experimental conditions, the contribution corresponding to the C- odd interference of the Borsellino and the $\gamma - e$ diagrams becomes zero. It is convenient to express the phase space of the recoil electron in terms of the invariant variables

$$\frac{d^3 p_2}{E_2} = \frac{d(-q^2)dQ^2 d\phi}{4(kp)} = \frac{d\Gamma}{4(kp)}, \quad d\Gamma = d\Phi d\phi,$$

where $q^2 = (p - p_2)^2$, $Q^2 = (p_1 + p_3)^2 = (k + q)^2$ is the square of the invariant mass of the produced electron-positron pair, ϕ is the azimuthal angle of the recoil electron (i.e., the angle between the photon polarization vector $\vec{e}_1$ and the plane containing the initial-photon and recoil-electron momenta, Fig. 2).

The limits of the integration over the Q^2 and q^2 variables are defined by the following relations

$$4m^2 \le Q^2 \le (\sqrt{W^2} - m)^2, \quad x_- \le -q^2 \le x_+, \quad W^2 = (k + p)^2 = m^2 + 2m\omega, \tag{11}$$

$$x_\pm = \frac{d}{W^2}(2d + Q^2) - Q^2 \pm \frac{d}{W^2}\sqrt{(2d - Q^2)^2 - 4m^2 Q^2};$$

$$4m^2 \le Q^2 \le -\frac{q^2}{m}(\omega\sqrt{1 - 4\frac{m^2}{q^2}} - m - \omega), \quad x_-(Q^2 = 4m^2) \le -q^2 \le x_+(Q^2 = 4m^2),$$

where ω is the photon-beam energy in the laboratory system. The accessible region of the Q^2 and q^2 variables is shown in Fig. 3.

Therefore, the distribution over the recoil-electron variables can be written as a sum of two contributions

$$\frac{d\sigma}{d\Gamma} = \frac{d\sigma(B)}{d\Gamma} + \frac{d\sigma(C)}{d\Gamma}, \tag{12}$$

where the first (second) term is the contribution of the Borsellino ($\gamma - e$) diagrams.
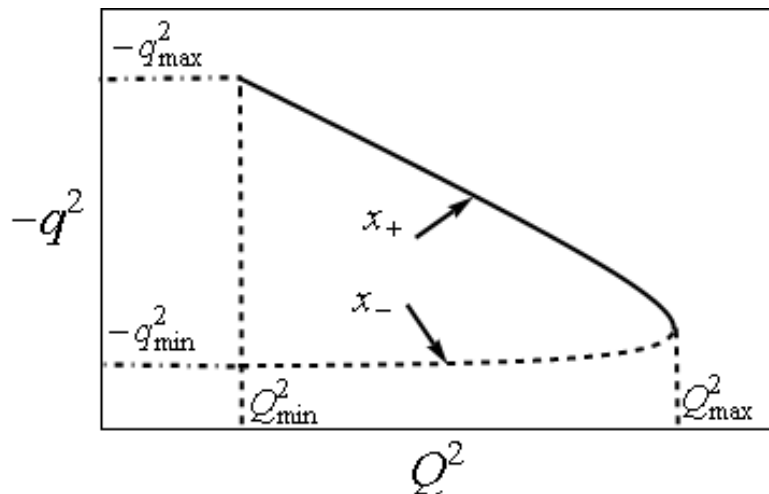

Fig 3. The allowed domain of the variables q^2 and Q^2.

THE BORSELLINO CONTRIBUTION

The tensor $T_{\mu\nu}(B)$, which describes the contribution of the Borsellino diagrams, can be represented as a product of two tensors of the second and fourth rank

$$T_{\mu\nu}(B) = t_{\lambda\rho}(B)t_{\mu\nu\lambda\rho}(B), \tag{13}$$

where the current tensor $t_{\lambda\rho}(B)$ describes the transition $e^-(p) \to \gamma^*(q) + e^-(p_2)$ and the tensor $t_{\mu\nu\lambda\rho}(B)$ describes the process $\gamma(k) + \gamma^*(q) \to e^-(p_1) + e^+(p_3)$.

The part of the distribution, caused by the Borsellino diagrams, can be written as

$$\frac{d\sigma(B)}{d\Gamma} = \frac{\alpha^3}{16\pi^2 d^2} \frac{1}{q^4} \Sigma(B), \tag{14}$$

where we introduce

$$\Sigma(B) = \rho_{\mu\nu}^{\gamma} Q_{\mu\nu\lambda\rho} t_{\lambda\rho}(B), \quad Q_{\mu\nu\lambda\rho} = \int t_{\mu\nu\lambda\rho}(B) \frac{d^3 p_1 d^3 p_3}{2E_1 2E_3} \delta^{(4)}(k+q-p_1-p_3). \tag{15}$$

The Borsellino tensor $t_{\mu\nu\lambda\rho}(B)$ in the case of unpolarized electron-positron pair was calculated in Ref. [15]. Note that the expression for this tensor in this paper contains some misprints. Correct expression has the following form

$$t_{\mu\nu\lambda\rho}(B,0) = t_{(\mu\nu)(\lambda\rho)}(B) + t_{[\mu\nu][\lambda\rho]}(B), \tag{16}$$

where we use the index notation $(\alpha\beta)$ ($[\alpha\beta]$) to emphasize the symmetry (antisymmetry) under permutation of the indices α and β. Note that the first tensor, which is symmetric, contributes in the case of unpolarized or linearly polarized photon beam. The second tensor, which is antisymmetric, contributes in the case of a circularly polarized photon beam.

$$t_{(\mu\nu)(\lambda\rho)}(B) = \frac{2}{d_1 d_3} \{ g_{\lambda\rho}[(d_1 + d_3)^2 g_{\mu\nu} - d_1 d_3 q^2 e_{\mu}^{(31)} e_{\nu}^{(31)}] - 2d_1 d_3 (1 + \hat{P}_{\mu\nu}) g_{\lambda\nu} g_{\mu\rho} - 2(p_1 p_3)_{\mu\nu} k_{\lambda} k_{\rho} + \tag{17}$$

$$(1 + \hat{P}_{\mu\nu} + \hat{P}_{\lambda\rho} + \hat{P}_{\mu\nu}\hat{P}_{\lambda\rho}) g_{\rho\nu}[k_{\lambda}(d_3 p_{1\mu} + d_1 p_{3\mu}) + d_1 d_3 (p_{1\lambda} - p_{3\lambda}) e_{\mu}^{(31)}] + [d_3 (p_1 e^{(31)})_{\mu\nu} (kp_3)_{\lambda\rho} - d_1 (p_3 e^{(31)})_{\mu\nu} (kp_1)_{\lambda\rho}] -$$

$$- g_{\mu\nu}[(d_1 + d_3)(kp_1)_{\lambda\rho} + (d_1 + d_3)(kp_3)_{\lambda\rho} - 2(m^2 + (p_1 p_3)) k_{\lambda} k_{\rho}] + 2d_1 d_3 e_{\mu}^{(31)} e_{\nu}^{(31)} (p_1 p_3)_{\lambda\rho} \},$$

$$t_{[\mu\nu][\lambda\rho]}(B) = \frac{2}{d_1 d_3} \{ (1 - \hat{P}_{\lambda\rho})[(d_1^2 + d_3^2) g_{\mu\lambda} g_{\nu\rho} + \frac{(d_1^2 p_{3\mu} - d_3^2 p_{1\mu}) k_{\rho}[p_1 p_3]_{\mu\nu}}{d_1 d_3}] + \tag{18}$$

$$+ (1 - \hat{P}_{\mu\nu} - \hat{P}_{\lambda\rho} + \hat{P}_{\mu\nu}\hat{P}_{\lambda\rho})[g_{\mu\rho} e_{\nu}^{(31)}(d_3^2 p_{1\mu} - d_1^2 p_{3\mu}) +$$

$$+ \frac{d_1^2 - (d_1 - d_3)(m^2 + (p_1 p_3))}{d_1} g_{\nu\alpha} k_{\rho} p_{1\mu} + \frac{d_3^2 - (d_3 - d_1)(m^2 + (p_1 p_3))}{d_3} g_{\nu\alpha} k_{\rho} p_{3\mu}] \},$$

where we use notation $(ab)_{\lambda\rho} = a_{\lambda} b_{\rho} + b_{\lambda} a_{\rho}$ and $[ab]_{\alpha\beta} = a_{\alpha} b_{\beta} - a_{\beta} b_{\alpha}$.

The tensor $Q_{\mu\nu\lambda\rho}$ was calculated in Ref. [8] for the case of $k^2 \neq 0$ using the method of the invariant integration. The expression for this tensor in the case of $k^2 = 0$ is given in Ref. [9] and it can be written as

$$Q_{\mu\nu\lambda\rho} = 2\pi\beta[D_1 g_{\mu\lambda} g_{\nu\rho} + D_2 g_{\lambda\rho} g_{\mu\nu} + D_3 g_{\nu\lambda} g_{\mu\rho} + \frac{D_4}{a^2} g_{\mu\nu} k_{\lambda} k_{\rho} + \frac{D_5}{a^2} g_{\lambda\rho} q_{\mu} q_{\nu} + \tag{19}$$

$$+ \frac{D_6}{a^3}(g_{\lambda\mu} q_{\nu} k_{\rho} + g_{\nu\rho} q_{\mu} k_{\lambda}) + \frac{D_7}{a^3}(g_{\lambda\nu} q_{\mu} k_{\rho} + g_{\mu\rho} q_{\nu} k_{\lambda}) + \frac{D_8}{a^4} q_{\mu} q_{\nu} k_{\lambda} k_{\rho}],$$

where $\beta = (1 - 4m^2 / Q^2)^{1/2}$, $a = (kq)$ and the structure functions $D_1 - D_8$ have the following form

$$D_1 = -2 - \frac{Q^4}{4a^2} + \frac{Q^2}{2a^2}(6a - m^2) + \frac{L}{a^2}[m^2(Q^2 - 2a - m^2) + a(a - Q^2)], \tag{20}$$

$$D_2 = -\frac{Q^2}{4a^2}(3Q^2 - 4a + 2m^2) + \frac{L}{a^2}[a(a - Q^2 + 2m^2) + \frac{Q^4}{2} - m^4],$$

$$D_3 = -\frac{Q^2}{4a^2}(Q^2 + 4a + 2m^2) + \frac{L}{a^2}(a + m^2)(Q^2 - a - m^2),$$

$$D_4 = q^2(D_2 - \frac{Q^2 q^2}{a^2} + 2\frac{m^2 q^2}{a^2}L), \quad D_5 = 0, \quad D_6 = -a^2 D_1,$$

$$D_7 = -a^2 D_3, \quad D_8 = a^2(D_1 + D_3), \quad L = \frac{1}{\beta}ln\frac{1+\beta}{1-\beta}.$$

Unpolarized case.
In the case when all particles are unpolarized, we have

$$\Sigma(B;0) = \frac{1}{2}(e_{1\mu}e_{1\nu} + e_{2\mu}e_{2\nu})t_{\lambda\rho}(B;0)Q_{\mu\nu\lambda\rho}. \tag{21}$$

The current tensor in the case of unpolarized initial electron is given by

$$t_{\lambda\rho}(B;0) = q^2 g_{\lambda\rho} + 2(pp_2)_{\lambda\rho}. \tag{22}$$

Performing the contraction of the tensors in the expression (21), one can obtain

$$\Sigma(B;0) = -2\pi\beta\{2(q^2 + 2m^2)D_2 + 4dd_2\frac{1}{a^2}D_4 + (D_1 + D_3)[2m^2 + \frac{d^2 + d_2^2}{a^2}q^2]\}. \tag{23}$$

A similar expression was calculated in Ref. [21] for the case of the lepton pair photoproduction on a proton target, $\gamma p \rightarrow l^+l^- p$, taking into account the Bethe-Heitler mechanism. This process was proposed to test a lepton universality by detecting the recoil proton.

Note that the expression (23) for the unpolarized cross section, calculated by the authors in Ref. [9], is not correct. The reason is that they used for the unpolarized photon spin-density matrix the expression $g_{\mu\nu}/2$ and contracted it with the tensor $Q_{\mu\nu\lambda\rho}$. It is not correct procedure because the expression for the tensor $Q_{\mu\nu\lambda\rho}$ is not gauge invariant (here the terms proportional to k_μ and k_ν were omitted).

Linearly polarized photon beam.
In the case of the linearly polarized photon beam, we have

$$\Sigma(B;\xi) = \frac{1}{2}[\xi_1(e_{1\mu}e_{2\nu} + e_{2\mu}e_{1\nu}) + \xi_3(e_{1\mu}e_{1\nu} - e_{2\mu}e_{2\nu})]\,Q_{\mu\nu\lambda\rho}\,t_{\lambda\rho}(B;0). \tag{24}$$

The contraction of these tensors in the above expression gives

$$\Sigma(B;\xi) = -4\pi\beta\frac{1}{a^2}(D_1 + D_3)(m^2a^2 + dd_2q^2)(\xi_1 sin2\phi + \xi_3 cos2\phi). \tag{25}$$

Circularly polarized photon beam.
In the case of the circularly polarized photon beam, we have

$$\Sigma(B;s,\xi_2) = -\frac{i}{2}\xi_2(e_{1\mu}e_{2\nu} - e_{2\mu}e_{1\nu})Q_{\mu\nu\lambda\rho}t_{\lambda\rho}(B;s). \tag{26}$$

The current tensor in the case of polarized initial electron is given by

$$t_{\lambda\rho}(B;s) = 2im < \lambda\rho qs >, \tag{27}$$

where s is the polarization 4-vector of the initial electron which satisfies the following conditions: $(ps) = 0$, $s^2 = -1$. In the laboratory system this vector has the form: $s = (0, \vec{s})$, where the unit vector $\vec{s}$ is determined by the polar and azimuthal angles θ^* and ϕ^*, respectively.

The contraction of these tensors in the above expression gives

$$\Sigma(B; s, \xi_2) = 4\pi\beta m \xi_2 (D_1 - D_3)[< e_1 e_2 qs > - \frac{1}{a}((qe_1) < ke_2 qs > -(qe_2) < ke_1 qs >)]. \tag{28}$$

As follows from this expression, the electron polarization vector normal to the plane $(\vec{k}, \vec{p}_2)$ does not contribute to the polarization observable. Indeed, let us choose $s_\mu^N \sim < \mu k p p_2 >$ (in the laboratory system we have $s_\mu^N = (0, \vec{s}^N)$, where $\vec{s}^N \sim (\vec{k} \times \vec{p}_2)$), then we have $< e_1 e_2 qs^N >= 0$ and $(qe_1) < ke_2 qs^N >= (qe_2) < ke_1 qs^N >$. Thus, only components of the electron polarization vector which belong to the plane $(\vec{k}, \vec{p}_2)$ give nonzero contribution to the polarization observables, namely they are s_z and the following combination $s_x \cos\phi + s_y \sin\phi$.

In the chosen coordinate system we can write

$$\Sigma(B; s, \xi_2) = 2\pi\beta\xi_2 (D_1 - D_3)[2m \,|\, \vec{p}_2 \,|\, \sin\theta(s_x \cos\phi + s_y \sin\phi) + (q^2 \frac{d + d_2}{a} + 2m^2 \frac{a}{d})s_z]. \tag{29}$$

Note that if the electron polarization vector is parallel or antiparallel to the photon beam momentum, then the cross section is not dependent on the azimuthal angle.

THE $\gamma - e$ CONTRIBUTION

The tensor $T_{\mu\nu}(C)$ can be represented as a product of two tensors of the second and fourth rank

$$T_{\mu\nu}(C) = t_{\lambda\rho}(C)t_{\mu\nu\lambda\rho}(C), \tag{30}$$

where the current tensor $t_{\lambda\rho}(C)$ describes the transition $\gamma^*(Q) \to e^+(p_3) + e^-(p_1)$ and the tensor $t_{\mu\nu\lambda\rho}(C)$ describes the process $\gamma(k) + e^-(p) \to \gamma^*(Q) + e^-(p_2)$.

We consider the case when the produced electron-positron pair is unpolarized. Then the current tensor is given by

$$t_{\lambda\rho}(C) = -2Q^2 g_{\lambda\rho} + 4(p_1 p_3)_{\lambda\rho}. \tag{31}$$

The part of the distribution, caused by the $\gamma - e$ diagrams, can be written as

$$\frac{d\sigma(C)}{dq^2 dQ^2 d\phi} = \frac{\alpha^3}{16\pi^2 d^2 Q^4} \rho_{\mu\nu}^\gamma t_{\mu\lambda\nu\rho}(C)C_{\lambda\rho}, \tag{32}$$

where we introduce

$$C_{\lambda\rho} = \int t_{\lambda\rho}(C) \frac{d^3 p_1 d^3 p_3}{2E_1 2E_3} \delta^{(4)}(Q - p_1 - p_3). \tag{33}$$

Taking into account that $Q_\lambda C_{\lambda\rho} = Q_\rho C_{\lambda\rho} = 0$ and that the tensor $C_{\lambda\rho}$ depends only on one variable Q_μ, we can write the general form for the tensor $C_{\lambda\rho}$ as

$$C_{\lambda\rho} = C(Q^2)(g_{\lambda\rho} - \frac{1}{Q^2} Q_\lambda Q_\rho). \tag{34}$$

The function $C(Q^2)$ can be easily calculated in the c.m.s. of the electron-positron pair. As a result we obtain

$$C(Q^2) = -\frac{2\pi}{3}\beta(Q^2 + 2m^2). \tag{35}$$

Write down the expression for the distribution, caused by the $\gamma - e$ diagrams, in the form

$$\frac{d\sigma(C)}{d\Phi} = \frac{\alpha^3}{16\pi^2 Q^4} \frac{C(Q^2)}{d^2} \Sigma(C), \tag{36}$$

where

$$\Sigma(C) = \rho_{\mu\nu}^{\gamma} (g_{\lambda\rho} - \frac{1}{Q^2} Q_\lambda Q_\rho) t_{\mu\nu\lambda\rho}(C). $$

Unpolarized case.
In the case when all particles are unpolarized, we have

$$\Sigma(C;0) = \frac{1}{2}(e_{1\mu}e_{1\nu} + e_{2\mu}e_{2\nu})(g_{\lambda\rho} - \frac{1}{Q^2} Q_\lambda Q_\rho) t_{\mu\nu\lambda\rho}(C;0). \tag{37}$$

The tensor $t_{\mu\nu\lambda\rho}(C)$, caused by the $\gamma - e$ diagrams, in the case of unpolarized particles has the following expression (we present here only symmetrical (over the λ, ρ indices) part of this tensor since the antisymmetrical part does not contribute in the case when the produced electron-positron pair is unpolarized)

$$t_{(\mu\nu)(\lambda\rho)}(C;0) = \frac{1}{dd_2} \{ g_{\lambda\rho}[(d-d_2)^2 g_{\mu\nu} + dd_2 Q^2 e_\mu^{(20)} e_\nu^{(20)}] + 2dd_2(1+\hat{P}_{\mu\nu})g_{\lambda\nu}g_{\mu\rho} + 2(pp_2)_{\mu\nu} k_\lambda k_\rho + \tag{38}$$

$$+(1+\hat{P}_{\mu\nu}+\hat{P}_{\lambda\rho}+\hat{P}_{\mu\nu}\hat{P}_{\lambda\rho})g_{\rho\nu}[-k_\lambda(dp_{2\mu}+d_2 p_\mu) + N(p_\lambda + p_{2\lambda})e_{1\mu}] - N[\frac{1}{d_2}(p_2 e_1)_{\mu\nu}(kp)_{\lambda\rho} + \frac{1}{d}(pe_1)_{\mu\nu}(kp_2)_{\lambda\rho}] -$$

$$-g_{\mu\nu}[(d_2-d)(kp_2)_{\lambda\rho} + (d-d_2)(kp)_{\lambda\rho} - 2(m^2-(pp_2))k_\lambda k_\rho] + 2dd_2 e_\mu^{(20)} e_\nu^{(20)}(pp_2)_{\lambda\rho}\},$$

where $\hat{P}_{\mu\nu}$ is the $\mu \leftrightarrow \nu$ permutation operator, the averaging over the initial electron spin is taken into account in this tensor.

Performing the contraction of the tensors in the expression (37), one can obtain

$$\Sigma(C;0) = -\frac{1}{dd_2}\{2(d^2+d_2^2) + (Q^2+2m^2)[q^2 + \frac{m^2}{dd_2}(d-d_2)^2]\}. \tag{39}$$

Linearly polarized photon beam.
In the case of the linearly polarized photon beam, we have

$$\Sigma(C;\xi) = \frac{1}{2}[\xi_1(e_{1\mu}e_{2\nu} + e_{2\mu}e_{1\nu}) + \xi_3(e_{1\mu}e_{1\nu} - e_{2\mu}e_{2\nu})](g_{\lambda\rho} - \frac{1}{Q^2} Q_\lambda Q_\rho) t_{\mu\nu\lambda\rho}(C;0). \tag{40}$$

The contraction of these tensors in the above expression gives

$$\Sigma(C;\xi) = -\frac{1}{dd_2}(Q^2+2m^2)[q^2 + \frac{m^2}{dd_2}(d-d_2)^2](\xi_1 sin2\phi + \xi_3 cos2\phi). \tag{41}$$

Circularly polarized photon beam.
The tensor $t_{\mu\nu\lambda\rho}(C;s)$, caused by the $\gamma - e$ diagrams, in the case of the polarized initial electron has the following expression

$$t_{\mu\nu\lambda\rho}(C;s) = \frac{im}{2d^2 d_2^2}\{4dd_2(p_\lambda p_\rho + p_{2\lambda} p_{2\rho}) - 2(d^2+d_2^2)(pp_2)_{\lambda\rho} - [Q^2(d+d_2)^2 - 2d(d^2-d_2^2)]g_{\lambda\rho}\} <\mu\nu ks> - \tag{42}$$

$$-\frac{im}{dd_2^2} <\mu\nu kq> [-dd_2(se^{(20)})_{\lambda\rho} + (d+d_2)(p_2 s)g_{\lambda\rho}] -$$

$$-\frac{im}{2d^2 d_2^2}(1+\hat{P}_{\lambda\rho}) <\mu\nu\rho k>[d(d+d_2)(Q^2+2d_2-2d)s_\lambda - 2(d(p_2 s) + d_2(ks))(d_2 p_{2\lambda} - dp_\lambda)].$$

The contraction of this tensor with the tensor $C_{\lambda\rho}$ leads to the following expression (we omit here the terms proportional to k_μ and k_ν since they do not contribute to the observables)

$$S_{\mu\nu}(C;s) = a_1 < \mu\nu ks > + a_2 < \mu\nu pk >,$$ (43)

where we introduce

$$a_1 = -im\frac{C(Q^2)}{d^2 d_2^2}[4dd_2(d-d_2) - d_2 Q^2(3d+d_2) - 2m^2(d-d_2)^2],$$

$$a_2 = 2im\frac{C(Q^2)}{d_2 d^2}(d-d_2)(p_2 s).$$

From the formula (43) one can conclude that if the electron polarization vector is perpendicular to the plane $(\vec{k}, \vec{p}_2)$ then it does not contribute to the polarization observable. The coefficient $a_2 = 0$ since $(p_2 s^N) = 0$ and the expression $<\mu\nu ks^N> \sim k_\mu(dp_{2\nu} - d_2 p_\nu) + k_\nu(d_2 p_\mu - dp_{2\mu})$ and it also does not contribute to the polarization effects. Thus, only components of the electron polarization vector which belong to the plane $(\vec{k}, \vec{p}_2)$ give nonzero contribution to the polarization observables, namely, they are s_z and the following combination $s_x \cos\phi + s_y \sin\phi$.

The contraction of this tensor with the photon spin-density matrix leads to non-zero result in the case when the photon beam is circularly polarized. The contraction is

$$\Sigma(C;s,\xi_2) = -\xi_2 \frac{1}{dd_2^2}\{m|\vec{p}_2|\sin\theta d_2(Q^2-q^2)(s_x \cos\phi + s_y \sin\phi) + s_z[m|\vec{p}_2|\cos\theta d_2(Q^2-q^2) +$$ (44)

$$+2dd_2(Q^2+q^2) + 2m^2(d-d_2)^2 + d_2(d_2-d)Q^2]\},$$

$$m|\vec{p}_2|\cos\theta = \frac{m^2}{2d}(Q^2-q^2) - \frac{q^2}{2}, \quad \vec{p}_2{}^2 \sin^2\theta = -\frac{1}{d^2}[m^2(d-d_2)^2 + dd_2 q^2],$$

where $s_i, i = x,y,z$ are the components of the electron polarization vector in the laboratory system $(s_z = \cos\theta^*, s_x = \sin\theta^* \cos\phi^*, s_y = \sin\theta^* \sin\phi^*)$. Note that if the electron polarization vector is parallel or antiparallel the photon beam momentum, then the cross section is not dependent on the azimuthal angle.

DIFFERENT DISTRIBUTIONS

The differential cross section of the reaction (1), in the case when the electron target and photon beam are polarized (the polarization state of the photon beam is described by the Stokes parameters) and the produced electron-positron pair is not detected, can be written as

$$\frac{d\sigma}{d\Gamma} = \frac{d\sigma^{(U)}}{d\Phi} + (\xi_1 \sin 2\phi + \xi_3 \cos 2\phi)\frac{d\sigma^{(L)}}{d\Phi} + \xi_2(s_x \cos\phi + s_y \sin\phi)\frac{d\sigma^{(CT)}}{d\Phi} + \xi_2 s_z \frac{d\sigma^{(CL)}}{d\Phi},$$ (45)

where the first term describes the unpolarized differential cross section of the reaction (1), the second term corresponds to the part of the differential cross section caused by the linearly polarized photon beam. The third (fourth) term corresponds to the part of the differential cross section caused by the circularly polarized photon beam and polarized initial electron in the case when the polarization vector of the target is orthogonal (parallel) to the photon momentum.

The azimuthal integration in (45) leads to multiplication of the $d\sigma^{(U)}$ and $d\sigma^{(CL)}$ by factor 2π, and to extract the part $d\sigma^{(CL)}$ we have to take the difference of the events number with two opposite values of z-component of the target electron polarization, s_z. To separate the part $d\sigma^{(CT)}$ at fixed electron polarization, it is enough to take difference between the events number in the forward $(0 < \phi < \pi/2, 3\pi/2 < \phi < 2\pi; \cos\phi > 0)$ and backward $(\pi/2 < \phi < 3\pi/2; \cos\phi < 0)$ hemispheres. To probe the part $d\sigma^{(L)}$, it is allowed to sum the events in the sectors

$(0 < \phi < \pi / 4, 7\pi / 4 < \phi < 2\pi)$; $(3\pi / 4 < \phi < 5\pi / 4)$ and   subtract   the   events   number   in   the   sectors $(\pi / 4 < \phi < 3\pi / 4); (5\pi / 4 < \phi < 7\pi / 4)$.

Double differential distributions

The unpolarized part of the differential cross section can be read as

$$\frac{d\sigma^{(U)}}{d\Phi} = \frac{d\sigma^{(U)}(B)}{d\Phi} + \frac{d\sigma^{(U)}(C)}{d\Phi}, \tag{46}$$

$$\frac{d\sigma^{(U)}(B)}{d\Phi} = \frac{\alpha^3}{2\pi} \frac{\beta}{q^4} \frac{1}{m^2\omega^2} (A - \frac{B}{r_1^2} L), \tag{47}$$

where the functions A and B are

$$A = m^2 + \frac{q^2}{2} + \frac{2}{r_1}(q^4 + 3m^2q^2 + 2m^4 - m\omega q^2) + \frac{2q^2}{r_1^2}[q^4 + m^2(2m^2 + 3q^2 + 2\omega^2) - \tag{48}$$

$$-4m\omega(m^2 + 2q^2)] + 8m\omega(2m\omega - q^2)(m^2 + 2q^2)\frac{q^2}{r_1^3} + 16m^2\omega^2 \frac{q^4}{r_1^4}(m^2 + 2q^2),$$

$$B = 8m^2\omega^2 \frac{q^2}{r_1^2}(q^4 + 6m^2q^2 - 4m^4) + 4m\omega \frac{q^2}{r_1}[4m^3(m+\omega) + 2mq^2(\omega - 3m) - q^4] + \tag{49}$$

$$+2r_1[4m^4 + q^4 + 2m(2m-\omega)q^2] + \frac{r_1^2}{2}(q^2 + 2m^2) + 4m(m-\omega)q^4 - 8m^6 + q^6 - 2m^2q^2(4m\omega - 2\omega^2),$$

$$\frac{d\sigma^{(U)}(C)}{d\Phi} = \frac{\alpha^3}{12\pi} \frac{\beta}{Q^4} \frac{1}{m^3\omega^3} \frac{1}{r_2}(Q^2 + 2m^2)\{2m^2(2\omega^2 - m^2) - \frac{m}{\omega}(2\omega^2 + m^2 + m\omega)Q^2 + \tag{50}$$

$$+\frac{m}{\omega}[m^2 + 2\omega(m+\omega)]q^2 + \frac{m}{2\omega}Q^2q^2 + \frac{1}{2}(1 - \frac{m}{\omega})Q^4 + \frac{1}{2}q^4 + \frac{2}{r_2}m^3\omega(Q^2 + 2m^2)\},$$

where $r_1 = Q^2 - q^2$ and $r_2 = 2m\omega + q^2 - Q^2$.

The part of the differential cross section caused by the linearly polarized photon beam can be read as

$$\frac{d\sigma^{(L)}}{d\Phi} = \frac{d\sigma^{(L)}(B)}{d\Phi} + \frac{d\sigma^{(L)}(C)}{d\Phi}, \tag{51}$$

$$\frac{d\sigma^{(L)}(B)}{d\Phi} = \frac{\alpha^3}{\pi} \frac{\beta}{q^4} \frac{1}{m\omega^2} \frac{1}{r_1^4}[\frac{1}{2}q^4 + m^2Q^2 + 2m^2(m^2 - q^2)L]\{(m+2\omega)q^4 + mQ^4 + 2q^2[2m\omega^2 - (m+\omega)Q^2]\}, \tag{52}$$

$$\frac{d\sigma^{(L)}(C)}{d\Phi} = \frac{\alpha^3}{12\pi} \frac{\beta}{Q^4} \frac{1}{m^3\omega^3} \frac{1}{r_2}(Q^2 + 2m^2)^2[-m^2 + \frac{2\omega + m}{2\omega}q^2 - \frac{m}{2\omega}Q^2 + 2m^3 \frac{\omega}{r_2}]. \tag{53}$$

The part of the differential cross section, caused by the circularly polarized photon beam and polarized initial electron in the case when its polarization vector is orthogonal to the photon momentum, can be written as

$$\frac{d\sigma^{(CT)}}{d\Phi} = \frac{d\sigma^{(CT)}(B)}{d\Phi} + \frac{d\sigma^{(CT)}(C)}{d\Phi}, \tag{54}$$

$$\frac{d\sigma^{(CT)}(B)}{d\Phi} = \frac{\alpha^3}{2\pi}\frac{\beta}{q^4}\frac{|\vec{p}_2|}{m\omega^2}\frac{1}{r_1}sin\theta[3Q^2 + q^2 - (Q^2 + q^2)L], \tag{55}$$

$$\frac{d\sigma^{(CT)}(C)}{d\Phi} = \frac{\alpha^3}{12\pi}\frac{\beta}{Q^4}\frac{|\vec{p}_2|}{m^2\omega^3}\frac{1}{r_2}sin\theta(Q^2 - q^2)(Q^2 + 2m^2). \tag{56}$$

The part of the differential cross section, caused by the circularly polarized photon beam and polarized initial electron in the case when its polarization vector is parallel to the photon momentum, can be written as

$$\frac{d\sigma^{(CL)}}{d\Phi} = \frac{d\sigma^{(CL)}(B)}{d\Phi} + \frac{d\sigma^{(CL)}(C)}{d\Phi}, \tag{57}$$

$$\frac{d\sigma^{(CL)}(B)}{d\Phi} = \frac{\alpha^3}{4\pi}\frac{\beta}{r_1 q^4}\frac{1}{m^2\omega^2}[3Q^2 + q^2 - (Q^2 + q^2)L][\frac{m}{\omega}Q^2 - q^2(1 + \frac{m}{\omega} - 4\frac{m\omega}{r_1})], \tag{58}$$

$$\frac{d\sigma^{(CL)}(C)}{d\Phi} = \frac{\alpha^3}{24\pi}\frac{\beta}{r_2 Q^4}\frac{1}{m^3\omega^3}(Q^2 + 2m^2)[\frac{m}{\omega}(1 + 2\frac{m\omega}{r_2})(Q^2 - q^2)^2 + q^4 - Q^4 + 4m\omega(Q^2 + q^2)]. \tag{59}$$

Distributions over Q^2 variable

Let us obtain the distributions over the square of the invariant mass of the produced electron-positron pair, i.e., over the Q^2 variable. To do this, it is necessary to integrate the distributions (46) - (59) over the q^2 variable. As a result, we have for the unpolarized part of the differential cross section

$$\frac{d\sigma^{(U)}}{dQ^2} = \frac{d\sigma^{(U)}(B)}{dQ^2} + \frac{d\sigma^{(U)}(C)}{dQ^2}, \tag{60}$$

$$\frac{d\sigma^{(U)}(B)}{dQ^2} = \frac{\alpha^3}{2\pi}\frac{\beta}{Q^6}\frac{1}{m^2\omega^2}[D_1 + D_2 Ln(\frac{V - \Delta}{V + \Delta}) + D_3 Ln[\frac{Q^2(m + 2\omega) + \omega(\Delta - V)}{Q^2(m + 2\omega) - \omega(\Delta + V)}]], \tag{61}$$

$$D_1 = \frac{\Delta}{3m\omega}\{Q^6 - 4m\omega Q^4 - 8m^3\omega Q^2 + 4m^2 Q^2(Q^2 + 7\omega^2) + 4m^4(Q^2 + 17\omega^2) +$$

$$+ \frac{L}{Q^2}[-Q^8 + m\omega Q^6 + 12m^3\omega Q^4 - 2m^2 Q^4(Q^2 + 8\omega^2) - 16\omega m^5 Q^2 + 4m^4 Q^2(Q^2 - 21\omega^2) + 8m^6(Q^2 + 17\omega^2)]\},$$

$$D_2 = 2m\{RQ^2(\omega - 3m) - 2m^3(5Q^2 + 4\omega^2) + \frac{L}{Q^2}[RQ^4(2m - \omega) +$$

$$+ 2m^2 RQ^2(3m - \omega) + 4m^3 Q^2(m^2 + 4m\omega + \omega^2) - 16m^5\omega^2]\},$$

$$D_3 = \frac{1}{2}[Q^4(Q^2 - 4m\omega + 12m^2) + 8m^2 Q^2(2m^2 - 2m\omega + \omega^2) + 32m^4\omega^2 -$$

$$- \frac{L}{Q^2}(Q^4 + 4m^2 Q^2 - 8m^4)(Q^4 - 4m\omega Q^2 + 4m^2 Q^2 + 8m^2\omega^2)],$$

$$\frac{d\sigma^{(U)}(C)}{dQ^2} = \frac{\alpha^3}{12\pi}\frac{\beta}{Q^4}\frac{Q^2 + 2m^2}{m^3\omega^3}\{\frac{\Delta}{(m + 2\omega)^2}[2m\omega(4Q^2 + \omega^2) + 2m^2(Q^2 + 9\omega^2) +$$

$$+ 16m^3\omega + 4m^4 + 7Q^2\omega^2] - [R(Q^2 + 2m^2) + 2m^2\omega^2]Ln(\frac{R + \Delta}{R - \Delta})\}, \tag{62}$$

where symbol *Ln* stands for natural logarithm and we introduce the following notation

$$\Delta = \sqrt{(Q^2 - 2m\omega)^2 - 4m^2 Q^2}, \ R = Q^2 - 2m\omega - 2m^2, \ V = Q^2 + 2m\omega.$$

The Q^2 distribution of the differential cross section caused by the linearly polarized photon beam can be read as

$$\frac{d\sigma^{(L)}}{dQ^2} = \frac{d\sigma^{(L)}(B)}{dQ^2} + \frac{d\sigma^{(L)}(C)}{dQ^2}, \tag{63}$$

$$\frac{d\sigma^{(L)}(B)}{dQ^2} = \frac{\alpha^3}{\pi} \frac{\beta}{Q^6} \frac{1}{m\omega^2} \{ \frac{\Delta}{6\omega} [Q^4 (L - \frac{Q^2}{4m^2}) + 2m(\frac{Q^2}{2m^2} + L)(\omega Q^2 + 2m^3 (1 + 17\frac{\omega^2}{Q^2}) - 4\omega m^2) - \tag{64}$$

$$-m^2 L(5Q^2 + 8\omega^2) + \frac{Q^2}{2}(Q^2 - 2\omega^2)] + 2m^2 [R(\omega + m(L-1)) - 2m^3 + 4m^2 \omega L(1 - \frac{m\omega}{Q^2})] Ln[\frac{Q^2 - 2m\omega - \Delta}{Q^2 - 2m\omega + \Delta}]\},$$

$$\frac{d\sigma^{(L)}(C)}{dQ^2} = \frac{\alpha^3}{12\pi} \frac{\beta}{Q^4} \frac{(Q^2 + 2m^2)^2}{m^3 \omega^3} (2\Delta - RLn(\frac{R+\Delta}{R-\Delta})). \tag{65}$$

The Q^2 distribution of the differential cross section, caused by the circularly polarized photon beam and polarized initial electron in the case when its polarization vector is orthogonal to the photon momentum, can be written as

$$\frac{d\sigma^{(CT)}}{dQ^2} = \frac{d\sigma^{(CT)}(B)}{dQ^2} + \frac{d\sigma^{(CT)}(C)}{dQ^2}, \tag{66}$$

$$\frac{d\sigma^{(CT)}(B)}{dQ^2} = \frac{\alpha^3 \beta}{4Q^2} \frac{1}{m^2 \omega^3} \{ Q^2 (1-L)\sqrt{m^2 + 2m\omega} + Q^2 [m - 3\omega + (\omega - m)L] + 2m\omega [\omega (3-L) + 2\sqrt{Q^2}(L-2)] \}, \tag{67}$$

$$\frac{d\sigma^{(CT)}(C)}{dQ^2} = -\frac{\alpha^3}{48} \frac{\beta}{Q^4} \frac{(Q^2 + 2m^2)}{m^2 \omega^2} \{ 8m^2 + \frac{1}{\sqrt{m}} (m + 2\omega)^{-3/2} [\Delta^2 + 4mR(m + 2\omega)] \}. \tag{68}$$

The Q^2 distribution of the differential cross section, caused by the circularly polarized photon beam and polarized initial electron in the case when its polarization vector is parallel to the photon momentum, can be written as

$$\frac{d\sigma^{(CL)}}{dQ^2} = \frac{d\sigma^{(CL)}(B)}{dQ^2} + \frac{d\sigma^{(CL)}(C)}{dQ^2}, \tag{69}$$

$$\frac{d\sigma^{(CL)}(B)}{dQ^2} = \frac{\alpha^3}{4\pi} \frac{\beta}{Q^2} \frac{1}{m^2 \omega^2} \{ 2\Delta(7 - 3L) + 2[2(Q^2 - 3m\omega) - L(Q^2 - 2m\omega)] Ln(\frac{V-\Delta}{V+\Delta}) + \tag{70}$$

$$+ \frac{1}{\omega} [\omega(L-3)(Q^2 - 4m\omega) + mQ^2 (1-L)] Ln[\frac{Q^2 (m+\omega) - 2m\omega^2 + \omega\Delta}{Q^2 (m+\omega) - 2m\omega^2 - \omega\Delta}]\},$$

$$\frac{d\sigma^{(CL)}(C)}{dQ^2} = \frac{\alpha^3}{12\pi} \frac{\beta}{Q^4} \frac{Q^2 + 2m^2}{m^3 \omega^2} \{ \frac{\Delta}{(m+2\omega)^2} [(m+3\omega)R + 4m(m+2\omega)^2] + 2m(m\omega + m^2 - Q^2) Ln(\frac{R+\Delta}{R-\Delta}) \}. \tag{71}$$

Distributions over q^2 variable

Let us obtain the distributions over the q^2 variable. To do this, it is necessary to integrate the distributions (46) - (59) over the Q^2 variable. As a result, we have for the unpolarized part of the differential cross section

$$\frac{d\sigma^{(U)}}{dq_m^2} = \frac{d\sigma^{(U)}(B)}{dq_m^2} + \frac{d\sigma^{(U)}(C)}{dq_m^2}, \; q_m^2 = -q^2, \qquad (72)$$

$$\frac{d\sigma^{(U)}(B)}{dq_m^2} = \frac{\alpha^3}{2\pi}\frac{1}{m^2\omega^2}\{\frac{1}{2q^4}(q^4 - 2m\omega q^2 + 4m^2q^2 + 4m^4)Ln(\frac{1+r}{1-r})Ln[\frac{m^3 Y}{q^2\omega^2}(1-\overline{\beta})^{-2}] + \qquad (73)$$

$$+\frac{1}{q^4}[2q^4 - 2m\omega q^2 + 5m^2 q^2 + 2m^4]LnG_1 + \frac{2}{q^4\overline{\beta}^5}Ln[\frac{2m^2(Y+m) - Yq^2(1-r\overline{\beta})}{2m^2(Y-m)}]$$

$$[8\frac{m^7}{q^4}(\omega - 4m - 2\frac{m}{q^2}(4m^2 + 2m\omega - \omega^2) - 4m^3\frac{\omega^2}{q^4}) + 4\frac{m^4}{q^2}(\omega^2 - 8m\omega + 11m^2) + q^2(q^2 - m\omega - 7m^2) + 4m^3(3\omega + m)] +$$

$$+2\overline{\beta}^{-5}ArcTanh(r\overline{\beta}^{-1})[1 - 64\frac{\omega^2 m^{10}}{q^{12}} - 2m\frac{\omega + 2m}{q^2} - \frac{8}{3}\frac{m^4}{q^6}(4\omega^2 + 24m\omega - 21m^2) + \frac{32}{3}\frac{m^8}{q^{10}}(7\omega^2 - 6m\omega - 12m^2) +$$

$$+\frac{8}{3}\frac{m^2}{q^4}(\omega^2 + 9m\omega - 6m^2) + \frac{16}{3}\frac{m^6}{q^8}(4\omega^2 + 3m\omega + 12m^2)] - r[2 - \frac{Y}{m} + 2\frac{m}{q^2}(3m - 3\omega - Y) + \frac{4}{3}\frac{m^2}{q^4}(3m^2 - \omega^2) +$$

$$+\frac{16}{3}\frac{m^5(m^2 + 2q^2)}{\omega q^6}(1-\overline{\beta})^{-3} - \frac{4}{3}\frac{m^3}{\omega q^6}(1-\overline{\beta})^{-2}(q^2(6q^2 - 11m\omega + 3m^2) - 4\omega m^3) + \frac{2}{3}\frac{m}{\omega q^4}(1-\overline{\beta})^{-1}(3q^4 - 21m\omega q^2 +$$

$$+m^2(4\omega^2 + 9q^2 - 6m\omega + 6m^2))] - Ln(\frac{1+r}{1-r})[\frac{1}{2mq^4}(q^2 + 2m^2)(Yq^2 - 2m^3) - \frac{8}{3}\frac{m^5}{\omega q^8(1-\overline{\beta})^3}(q^4 + 6m^2 q^2 - 4m^4) +$$

$$+2\frac{m^3}{\omega q^6}(1-\overline{\beta})^{-2}(q^2(q^2 - 2m\omega + 6m^2) - 4m^3(\omega + m)) + \frac{m}{\omega q^6}(1-\overline{\beta})^{-1}(-q^6 + 4m\omega q^4 + 4m^2 q^2(2m\omega - q^2 - \omega^2) + 8m^6)] -$$

$$-\frac{1}{q^4}(q^4 - 2m\omega q^2 + 4m^2 q^2 + 4m^4)[Li_2(\frac{1-r}{2}) - Li_2(\frac{1-r}{1-\overline{\beta}}) - Li_2(\frac{1-r}{1+\overline{\beta}}) + Li_2(\frac{1+r}{1+\overline{\beta}}) + Li_2(\frac{1+r}{1-\overline{\beta}}) - Li_2(\frac{1+r}{2})]\},$$

$$\frac{d\sigma^{(U)}(C)}{dq_m^2} = \frac{\alpha^3}{12\pi}\frac{1}{m^3\omega^3}\{\frac{r}{6m\omega y^3}[48\omega^2 m^8 + 96\omega m^7(\omega^2 - q^2) + 48m^6(3\omega^2 q^2 + \omega^4) + \qquad (74)$$

$$+4m^5(26\omega^3 q^2 + 40\omega^5 + 23\omega q^4) + 2m^4 q^2(11q^4 + 40\omega^2 q^2 + 120\omega^4) + 2\omega q^2 m^3(12\omega^4 + 70q^2\omega^2 + 7q^4) +$$

$$+q^4 m^2(-3q^4 + 40\omega^2 q^2 + 36\omega^4) + m\omega q^6(5q^2 + 18\omega^2) + 3\omega^2 q^8 + 3\overline{\beta}\omega q^2 y^3(\omega - m) + 12y\omega m^5\frac{(y + 2m^2)^2}{2m^2 + (\overline{\beta}-1)q^2}] -$$

$$-\frac{2}{3}\frac{rm^3}{\omega Y q^2 y^2}[\omega q^4(q^2 + 6m\omega) + 4\omega m^2 q^2(q^2 + 4\omega^2) + 2m^3(q^4 + 4q^2\omega^2 + 8\omega^4)] + \frac{1}{2\omega}[2m(m+\omega)^2 - \omega q^2]LnG_1 -$$

$$-\frac{LnG_2}{y^3\sqrt{y(y - 4m^2)}}[16\omega m^7(m - \omega)^2 - 32q^2 m^7(m + \omega) + 4m^4 q^4(2m^2 + 3q^2) - 8m^4\omega^4(5q^2 - 6m^2) +$$

$$+4m^4\omega^2 q^2(12m^2 + 13q^2) + 16m^5\omega^3(5q^2 - \omega^2) + 4\omega q^4 m^3(11m^2 - 11\omega^2 + 4q^2) - q^8(8m\omega + q^2) - 2m^2 q^6(13\omega^2 - q^2)]\},$$

where

$$\overline{\beta}^2 = 1 - \frac{4m^2}{q^2}, Y = m + \omega(1-\overline{\beta}), r = \sqrt{1 - \frac{4m^3}{Yq^2}}, y = q^2 + 2m\omega, G_1 = \frac{q^2}{2m^3}(1+r)Y - 1,$$

$$Li_2(x) = -\int_0^x \frac{dt}{t} ln(1-t) , \quad G_2 = \frac{1}{2m^2\omega}[2m^2 + q^2(\overline{\beta}-1)]^{-1}\{q^2Y[r\sqrt{y(y-4m^2)} + y - 2m^2] - 2ym^3\}.$$

The q^2 distribution of the differential cross section caused by the linearly polarized photon beam can be read as

$$\frac{d\sigma^{(L)}}{dq_m^2} = \frac{d\sigma^{(L)}(B)}{dq_m^2} + \frac{d\sigma^{(L)}(C)}{dq_m^2}, \tag{75}$$

$$\frac{d\sigma^{(L)}(B)}{dq_m^2} = \frac{\alpha^3}{\pi}\frac{1}{m\omega^2 q^4}\{-\frac{r}{6}[3q^2(m+\omega) + 4m\omega^2 - 3\frac{m^2\overline{\beta}}{\omega(1-\overline{\beta})^2}(q^2+2mY) + 8\frac{m^5}{q^2}(1-\overline{\beta})^{-2} + 4\frac{m^4}{\omega q^2}\frac{(q^2+2m^2)}{(1-\overline{\beta})^3}] +$$

$$+ m^3 LnG_1 + 2\frac{m^4(m^2-q^2)}{\omega q^2(1-\overline{\beta})^2}[\frac{8}{3}\frac{m^2}{q^2}(1-\overline{\beta})^{-1} - 1]Ln(\frac{1+r}{1-r}) + \frac{4}{3}\frac{\omega^2 m^3}{\overline{\beta}q^2}Ln[\frac{2m^2(Y+m) - Yq^2(1-r\overline{\beta})}{2m^2\omega(1-\overline{\beta})}]\}, \tag{76}$$

$$\frac{d\sigma^{(L)}(C)}{dq_m^2} = \frac{\alpha^3}{12\pi}\frac{1}{m^3\omega^3}\{-\frac{2m^2r}{6\omega y^3}[24\omega^2 m^5 + 48\omega m^4(\omega^2-q^2) + 24\omega^2 m^3(\omega^2+3q^2) + 2\omega q^2 m^2(23q^2+56\omega^2) + \tag{77}$$

$$+ mq^4(11q^2+94\omega^2) + 22\omega q^6 - \frac{3q^2 y^3}{2m^2}(m+\omega(1-\overline{\beta})) + 4ym^3\frac{mq^2+2y\omega}{m+\omega(1-\overline{\beta})} - 6y\omega m^2\frac{(y+2m^2)^2}{2m^2+q^2(\overline{\beta}-1)}] +$$

$$+ \frac{1}{\omega}(m^3+2m^2\omega-\omega q^2)LnG_1 - \frac{LnG_2}{y^3\sqrt{y(y-4m^2)}}[16\omega m^9 - 32m^8(q^2+\omega^2) - 16\omega m^7(2q^2+\omega^2) - 8m^6(q^4-4\omega^2 q^2-4\omega^4) +$$

$$+ 4\omega q^2 m^5(11q^2+16\omega^2) - 4m^4 q^2(4\omega^4-12\omega^2 q^2-3q^4) - 16\omega m^3 q^4(2\omega^2-q^2) - 2m^2 q^6(12\omega^2-q^2) - 8m\omega q^8 - q^{10}]\}.$$

The q^2 distribution of the differential cross section, caused by the circularly polarized photon beam and polarized initial electron in the case when its polarization vector is orthogonal to the photon momentum, can be written as

$$\frac{d\sigma^{(CT)}}{dq_m^2} = \frac{d\sigma^{(CT)}(B)}{dq_m^2} + \frac{d\sigma^{(CT)}(C)}{dq_m^2}, \tag{78}$$

$$\frac{d\sigma^{(CT)}(C)}{dq_m^2} = \frac{\alpha^3}{12\pi}\frac{1}{m^2\omega^3}\frac{1}{\sqrt{b(a+c)}}\{\frac{\overline{\beta}q^2}{3my}\frac{a+c}{a}(3ay+4m^2 q^2)K(\frac{a(b-c)}{b(a+c)}) + \tag{79}$$

$$+ \frac{2m^2}{3\omega y^2}\frac{a+c}{ac}E(\frac{a(b-c)}{b(a+c)})[3ab(3q^4+4m\omega(m\omega-2m^2+2q^2)) - yq^2(a(b+c)-bc)] -$$

$$- 4\frac{\omega\overline{\beta}}{y^2}q^2(2m^2+y)(4m^2-y)\Pi(\frac{(a+y)(b-c)}{(a+c)(b-y)}|\frac{a(b-c)}{b(a+c)}) + 2\frac{\overline{\beta}}{m^2}q^2[(m+\omega)q^2 - 2m^2\omega]\Pi(\frac{(c-b)}{(a+c)}|\frac{a(b-c)}{b(a+c)})\},$$

where K, E, and Π are the standard elliptic functions [22] and

$$a = -\frac{q^2}{m}(m+\omega+\omega\overline{\beta}), b = \frac{q^2}{m}(m+\omega-\omega\overline{\beta}), \quad c = 4m^2.$$

Note that we can not represent the analytic expression for the contribution $d\sigma^{(CT)}(B)/dq_m^2$ in terms of the elementary or known special functions.

The q^2 distribution of the differential cross section, caused by the circularly polarized photon beam and polarized initial electron in the case when its polarization vector is parallel to the photon momentum, can be written as

$$\frac{d\sigma^{(CL)}}{dq_m^2} = \frac{d\sigma^{(CL)}(B)}{dq_m^2} + \frac{d\sigma^{(CL)}(C)}{dq_m^2}, \tag{80}$$

$$\frac{d\sigma^{(CL)}(B)}{dq_m^2} = \frac{\alpha^3}{4\pi}\frac{1}{m^2\omega^2 q^4}\{\frac{rYq^2}{4m\omega}[q^2(7Y+8m-16\omega)-6m^3]-8q^2\overline{\beta}(m\omega-q^2)ArcTanh\frac{r}{(1-\overline{\beta})}+8q^2\frac{mY}{1-\overline{\beta}}(Ln(\frac{1+r}{1-r})-2r)-$$

$$-Ln(\frac{1+r}{1-r})[\frac{m^2}{\omega}(3m^3-4\omega q^2)+\frac{Yq^4}{2m\omega}(Y+2m-2\omega)+4m\omega q^2+q^2(q^2-2m\omega)(Ln[\frac{\omega^2 q^2(1-\overline{\beta})^2}{m^3 Y}]+4)]+ \tag{81}$$

$$+2q^2(q^2-2m\omega)[Li_2(\frac{1+r}{1-\overline{\beta}})-Li_2(\frac{1-r}{1-\overline{\beta}})+Li_2(\frac{1+r}{1+\overline{\beta}})-Li_2(\frac{1-r}{1+\overline{\beta}})+Li_2(\frac{1-r}{2})-Li_2(\frac{1+r}{2})]\},$$

$$\frac{d\sigma^{(CL)}(C)}{dq_m^2} = \frac{\alpha^3}{24\pi}\frac{1}{m^3\omega^3}\{\frac{1}{\omega}[q^2(\omega+m)-2m\omega^2]LnG_1+4\frac{m\omega}{\sqrt{y(y-4m^2)}}[q^2+m(\omega-3m)- \tag{82}$$

$$-40\frac{\omega m^7}{y^3}+4\frac{m^5}{y^2}(\omega+2m)+2\frac{m^3}{y}(2\omega-3m)]Ln[\frac{\omega G_2[2m^2+q^2(\overline{\beta}-1)]}{Yq^2-my}]-r[\frac{\omega-m}{m\omega}(4m^3-Yq^2)+80\frac{\omega^2 m^6}{y^3}+$$

$$+\frac{16}{3}\frac{\omega m^4}{y^2}(\omega-3m)-\frac{4}{3}\frac{\omega m^2}{y}(5\omega-7m)+\frac{5}{3}\frac{(y\omega+mq^2)}{\omega}+8\frac{\omega^2 m^5}{y^2}\frac{y+2m^2}{Yq^2-my}+\frac{4}{3}\frac{m^3}{Y}(1+\frac{m}{\omega}+2\frac{m\omega}{y^2}(y-2m^2))]\}.$$

RESULTS AND DISCUSSION

There are a few reasons to investigate process of the triplet photoproduction in the framework of a more elaborative approach. Our analysis of the triplet production is caused mainly by the search for a physics beyond SM in the frame of the project IRIDE [19]. It is assumed that there is a new light particle (U-boson [20] which is one of the possible dark-matter candidate) that does not interact with the matter fields of the SM but can mix with a photon.

In the last time there were a number of the experiments on the measuring of the electron-positron invariant mass distributions in different processes. The inclusive dielectron spectra, measured by the HADES (Darmstadt) in the collisions of the 3.5 GeV proton with the hydrogen, niobium and other targets, were presented in the paper [23]. The mass range M(U)=20 – 550 MeV has been investigated. The results of a search for a dark photon in the reaction $e^+e^- \to \gamma U, U \to e^+e^-, \mu^+\mu^-$ using the BABAR detector were given in [24]. The dark photon masses in the range 0.02 - 10.2 GeV were investigated. Strong constraints on sub-GeV dark photon from SLAC beam-dump experiment were given in the paper [25]. Similar experiments were performed at KEK and Orsay [26]. The physics motivation for a search of the dark photon at JLab are presented in [27]. This is not a complete list of the current and planned experiments to search for a dark photon. A review of the theoretical and experimental activity related to the search for the particles in various scenarios of the physics beyond the SM can be found in Ref. [28].

We think that the measurement of the distribution over the invariant mass of the created electron-positron pair in the process (1) would be a good method to search for a light dark photon. The contribution of the Borsellino diagrams is a background in search of this effect, so, it is necessary to separate the contribution of the Compton-like diagrams (Fig. 1b) when the scattered virtual photon converts into the electron-positron pair and where the signal from the dark photon may be measured. Because this contribution, in contrast to the Borsellino one, decreases with the growth of the photon-beam energy, it is reasonable, in such investigation, to restrict yourselves to the low and intermediate photon-beam energies. Besides, one has to have the precise knowledge of the background due to the double-photon e^+e^- - system (in fact the contribution of the Borsellino diagrams) and to try to find the kinematic regions where this background is smaller or the same order as the Compton contribution.

The next reason is the investigation of the possibility of determining the circular polarization degree of a high energy photon by measuring the asymmetry in the triplet production by a circularly polarized photon beam on a polarized electron target. It is necessary also to analyze the influence of the $(\gamma - e^-)$ diagrams contribution on the calculated observables.

The authors of Ref. [9] calculated the cross section asymmetry caused by the azimuthal angle of the recoil electrons in the reaction (1) for the case of the linearly polarized photons. They suggested to use this effect for the analysis of the photon beam polarization. The authors took into account only the Borsellino diagrams, and, up to now, there are no calculations beyond this approach. We consider the influence of the $(\gamma - e^-)$ diagrams contribution on the

asymmetry as a function of the q_m^2 variable and calculate its dependence on the Q^2 variable.
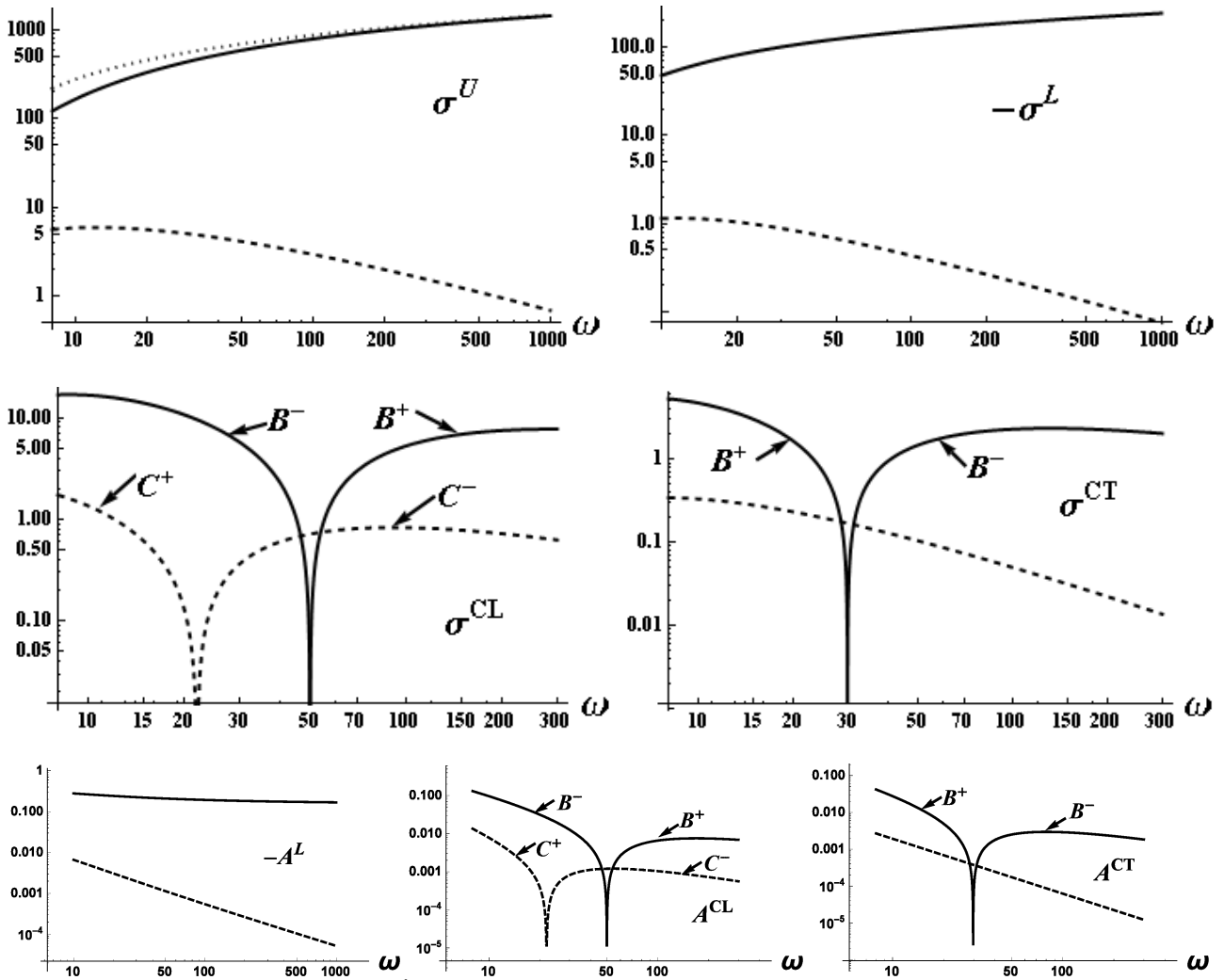

Fig. 4. The parts of the cross section (45) (the first and second rows) integrated numerically over all the phase space except the azimuthal angle, in μb, as a function of the photon-beam energy ω, in MeV. The solid (dashed) curves correspond to the contribution of the Borsellino ($\gamma - e^-$) diagrams. The asymmetries (84) are shown in the third row. The dotted curve in the upper left panel is the nondecreasing (with the increase of the photon-beam energy) contribution caused by the Borsellino diagrams that is defined by Eq.(83). The upper indices in the second and third rows ($\pm$) denote the positive (+) or negative (-) value of the corresponding observables. For the negative value of the observable the logarithm of its modulus is shown.

In Fig. 4 we present the integrated over Q^2 and q_m^2 (in the limits (11)) parts of the cross section, given in the r.h.s. of Eq. (45), and corresponding polarization asymmetries. They are obtained by the numerical integration over Q^2 of our analytic distributions, derived in subsection "Distributions over Q^2 variable" of the Section "DIFFERENT DISTRIBUTIONS". For unpolarized case we show also the well known asymptotic cross section (at large photon-beam energy $\omega \gg m$), caused by the Borsellino diagrams only, which in our normalization reads [29]

$$\sigma = \frac{\alpha^3}{2\pi m^2}(\frac{28}{9}\ln\frac{2\omega}{m} - \frac{218}{27}).$$ (83)

The asymmetries, as functions of the photon beam energy (Fig. 4), are defined as follows

$$A^I = \frac{\sigma^I}{\sigma^U}, I = L, CL, CT,$$ (84)

where σ^U is unpolarized cross section caused by a sum of the Borselino and ($\gamma - e^-$) contributions.

The differential asymmetries, as functions of the q_m^2 or Q^2 variables and photon-beam energy, are defined as

$$A_{q_m^2}^I = \frac{d\sigma^I / dq_m^2}{d\sigma^U / dq_m^2}, \quad A_{Q^2}^I = \frac{d\sigma^I / dQ^2}{d\sigma^U / dQ^2}. \tag{85}$$

We see that the ($\gamma - e^-$) diagrams contribute to the unpolarized part at $100\,\text{MeV} < \omega < 200\,\text{MeV}$ on the level of a few μb (remind that we consider the ϕ-distribution, and integration over the angle ϕ increases the unpolarized part σ^U, as well as the polarization-dependent part σ^{CL}, by a factor 2π). The Borsellino contribution to the total cross section is more than two orders larger.

As regards the polarization-dependent parts at these energies, the ($\gamma - e^-$) contribution is the largest for the circularly polarized photon and the longitudinally polarized (along the direction (**q**)) target electron (CL-part). It is negative and amounts to about 0.5 μb in the absolute value at $\omega = 100\,\text{MeV}$, which very slowly decreases with the growth of the photon-beam energy. If the the target electron is polarized transversally (in the plane (**q**, **p**$_2$)) (CT-part), the corresponding part of the cross section is positive and equals to about $5 \cdot 10^{-2} \mu b$ at $\omega = 100\,\text{MeV}$ and decreases up to $2 \cdot 10^{-2} \mu b$ at $\omega = 200\,\text{MeV}$. In the first case, the Borsellino contribution exceeds the ($\gamma - e^-$) one (in absolute value) by an order, and in the second case – by two orders. The part, caused by the linear polarization of the photon (L-part), is negative for both the ($\gamma - e^-$) and Borsellino contributions (this agrees with previous calculations). The ($\gamma - e^-$) contribution is less than one percent of the Borsellino one at $\omega = 100\,\text{MeV}$ and decreases with the rise of the energy whereas the Borsellino contribution increases.

Thus, to separate the effect due to the ($\gamma - e^-$) diagrams using the total cross section, even in the frame of the pure QED, the radiative corrections (RC) to the Borsellino contribution have to be taken into account. At present, we know such RC to the positron spectrum and to the total cross section in the Weizsacker-Williams approximation only [30] (in unpolarized case). This correction covers the region $q_m^2 \leq m^2$ and amounts to about one percent. It means that for our goal we have to compute RC more accurately and consider in the first order the contribution of the region of the $q_m^2 \sim$ a few tens of m^2 and even the leading (enhanced by a large logarithm) terms of the second order. Such calculations are absent at present.

The asymmetry A^L (caused by the linear polarization of the photon beam), as a function of the photon energy ω, is noticeable and depends weakly on ω. The contribution of the $\gamma - e^-$ diagrams is small ($\sim 1\%$ at $\omega \leq 10\,\text{MeV}$) and decreases rapidly as the photon energy increases. The asymmetry A^{CL} is of the order of $10-15\%$ in the region $\omega \leq 20\,\text{MeV}$ and decreases as a function of ω. The contribution of the $\gamma - e^-$ diagrams is less than 1% in the region $\omega \leq 10\,\text{MeV}$ and decreases very rapidly. The behavior of the asymmetry A^{CT} is similar to the asymmetry A^{CL} but it is somewhat less. The circular polarization of the photon beam can be determined, in principle, by means of the measurement of the asymmetry A^{CL} for the photon energies $\leq 20\,\text{MeV}$.

The main contribution to the triplet total cross section, given by Eq. (83), arises due to the region of a very small values of $q_m^2 \sim m^2$. To reduce this contribution kinematically, we have to select events with large values of $q_m^2 \gg m^2$. The different distributions over the q_m^2 variable (at large enough values of q_m^2) and the ratio R of the Borsellino contribution to the ($\gamma - e^-$) one are shown in Figs. 5, 6, and the polarization asymmetries defined by Eq. (84) are given in Fig. 7.

We see from Figs. 5, 6 that the ($\gamma - e^-$) contribution increases with the rise of q_m^2 whereas the Borsellino one decreases. Such behaviour ensures the suppression of the Borsellino contribution at large q_m^2 near its maximal possible values, where the corresponding parts of the cross section is determined, almost completely, by the ($\gamma - e^-$) contribution. The unpolarized part equals more than 0.1 μb at $\omega = 100\,\text{MeV}$ and two times smaller at $\omega = 200\,\text{MeV}$. At $\omega = 100\,\text{MeV}$ the CL-part reaches, in absolute value, 0.04 μb, the CT-part $- 0.001\,\mu b$ and the L-part – about 0.01 μb.
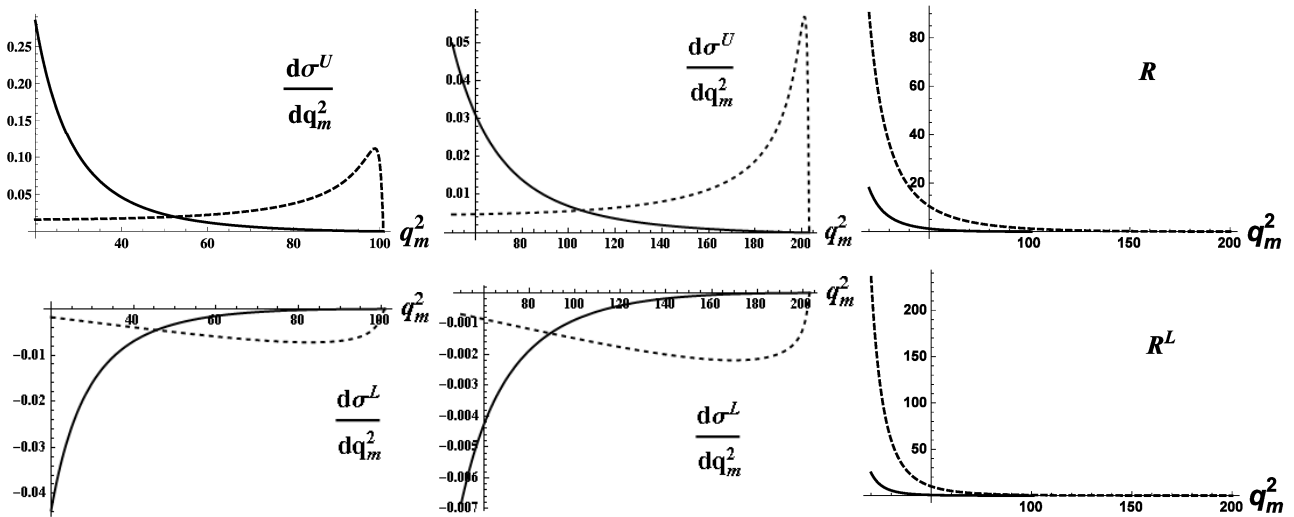
Fig.5. The parts of the differential cross section (in $\mu b \cdot \text{MeV}^{-2}$) for the photon-beam energy 100 MeV and 200 MeV versus q_m^2 (in MeV^2) integrated over all the possible values of the created pair invariant mass squared Q^2. The upper row is the polarization independent part, and the lower one corresponds to the linearly polarized photon. The solid curves in the left and middle panels describe the Borsellino contribution and the dashed curves – the ($\gamma - e^-$) one. In the right panels we show ratio R and R^L of the Borsellino contributions to the ($\gamma - e^-$) one at $\omega = 100$ MeV (solid curves) and 200 MeV (dashed curves).
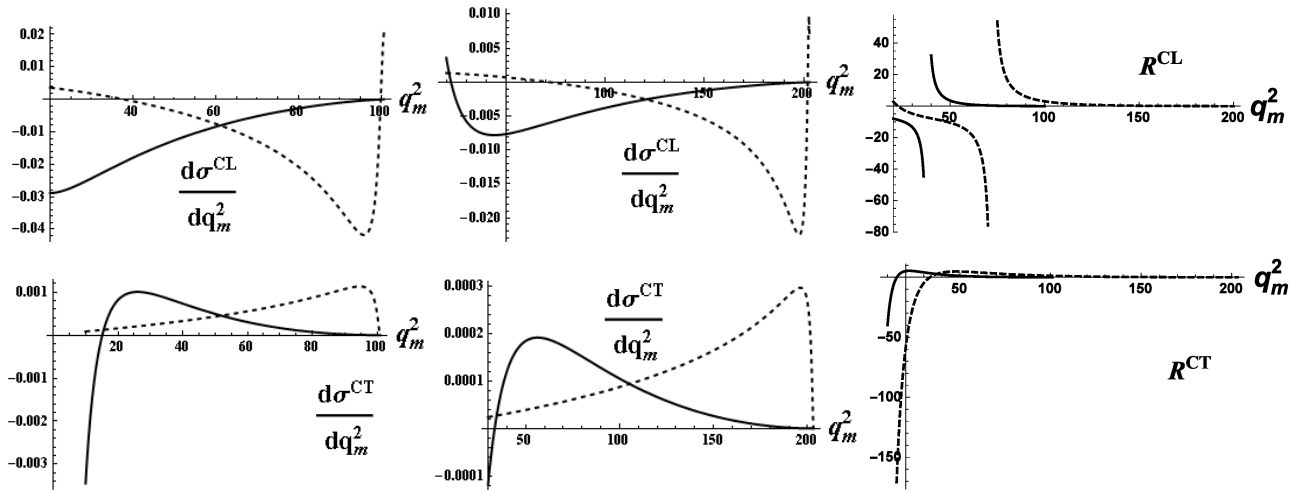

Fig 6. The same as in Fig. 5 but for the case of the circularly polarized photon and longitudinally (the upper row) and transversely (the lower row) polarized electron.
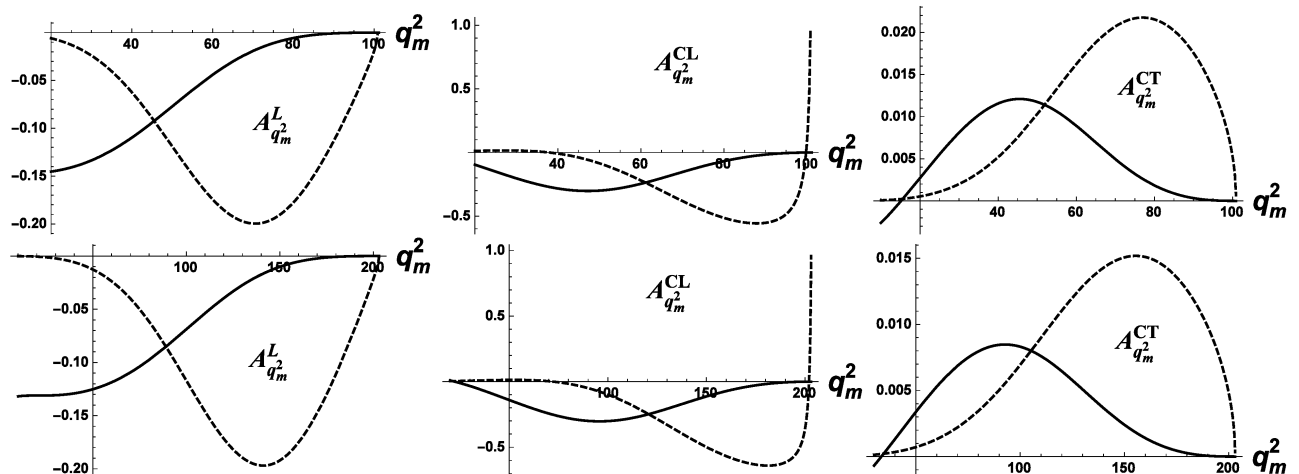

Fig 7. The differential asymmetries as function of the q_m^2 variable at $\omega = 100$ MeV (the upper row) and $\omega = 200$ MeV (the lower row). The solid (dashed) curves describe the Borsellino ($\gamma - e^-$) contribution.

The Fig. 7 shows that the asymmetry $A^L_{q^2_m}$ is of the order of $15-20\%$ in the region $q^2_m \leq 90(160)$ MeV^2 at $\omega = 100$ (200) MeV. The Borsellino contribution decreases and the $\gamma - e^-$ one increases. The asymmetry $A^{CL}_{q^2_m}$ is of the order of 40-50%. The $\gamma - e^-$ contribution is small in the region $q^2_m \leq 50(100)$ MeV^2 at $\omega = 100$ (200) MeV and beyond this region its contribution is dominated. The magnitudes of the asymmetry $A^{CT}_{q^2_m}$ is less than 1% in entire considered region. We see that the asymmetry $A^{CL}_{q^2_m}$ is appreciable and can be measured, in principle. So, it is possible to determine the circular polarization of the photon beam at more higher energies than for the case of the asymmetry A^{CL} since the general picture of the behavior of these asymmetries depends weakly on the photon energy.

To search for the deviation from SM due to the possible mixing of a photon with the light dark matter candidate (U-boson), it is necessary to study the distribution over the created pair invariant mass Q^2. In Figs.8-11 we show such distributions which derived by the integration over the restricted region of q^2_m, including the events with $q^2_m > 10, 20$ and 40 MeV^2 and analyse the corresponding effects. In contrast to the Borsellino contribution, the $(\gamma - e^-)$ one depends not very strong on the value of the q^2_m cut.

In Fig. 8 we show the unpolarized part of the cross section caused by the $(\gamma - e^-)$ diagrams with chosen restrictions and the ratio R^{-1} of the $(\gamma - e^-)$ to the Borsellino contributions. We see that for $\omega = 100$ MeV, even for the events with $q^2_m > 20$ MeV^2, there exist regions of the relative small and large values of Q^2 where the $(\gamma - e^-)$ contribution is greater than the Borsellino one (but the event number is larger at small Q^2). For the events with $q^2_m > 40$ MeV^2, this effect manifests itself more significantly. The more sizeable restriction on the minimal values of q^2_m is required at larger photon-beam energies to decrease the Borsellino contribution, as it is seen even for $\omega = 200$ MeV.
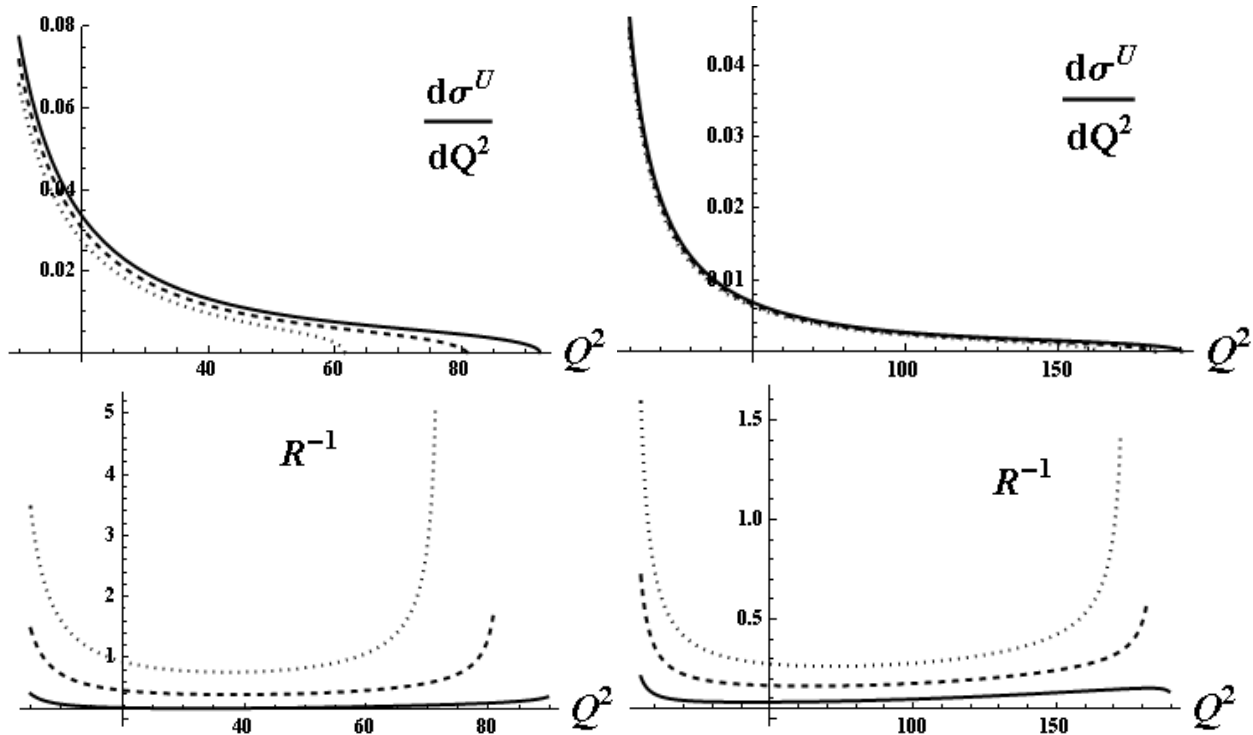

Fig 8. The $(\gamma - e^-)$ contribution to the polarization-independent part of the cross section as a function of Q^2, in $\mu b \cdot$ MeV^{-2}, at different restrictions on the event selection (the upper row) at $\omega = 100$ MeV (the left panel) and 200 MeV (the right panel). The solid line corresponds to the events with $q^2_m > 10$ MeV^2, the dashed line $- q^2_m > 20$ MeV^2 and the dotted one $- q^2_m > 40$ MeV^2. In the lower row we show the respective ratio R^{-1} of the $(\gamma - e^-)$ contribution to the Borsellino one.

In Figs. 9, 10 we show the effect caused by the restriction on the minimal values of q^2_m for the polarized parts of the cross section for both the $(\gamma - e^-)$ and Borsellino contributions. The corresponding polarization asymmetries, defined by Eq. (85), are given in Fig. 11. Again, we see that the $(\gamma - e^-)$ diagrams give the dominant contribution in the region of the large values of Q^2 and at large enough cuts on the q^2_m variable.
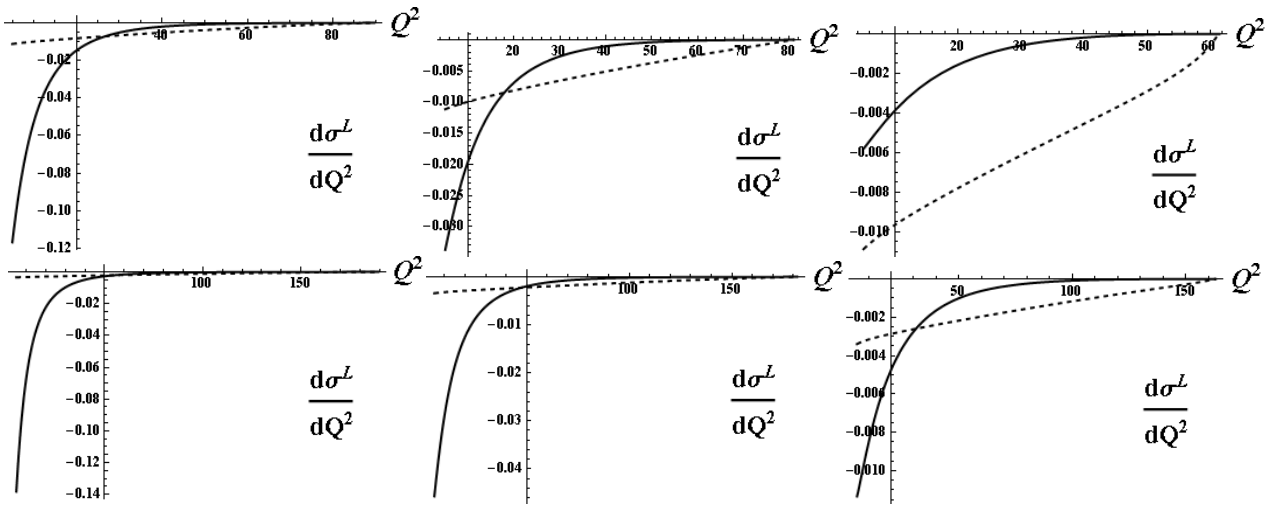
Fig 9. The part of cross section which depends on the linear polarization of the photon, in $\mu b \cdot \text{MeV}^{-2}$, for $\omega = 100$ MeV (the upper row) and $\omega = 200$ MeV (the lower row). The left (middle, right) panel corresponds to the events with $q_m^2 > 10$ (20, 40) MeV^2. The solid (dashed) line describes the Borsellino ($(\gamma - e^-)$) contribution.
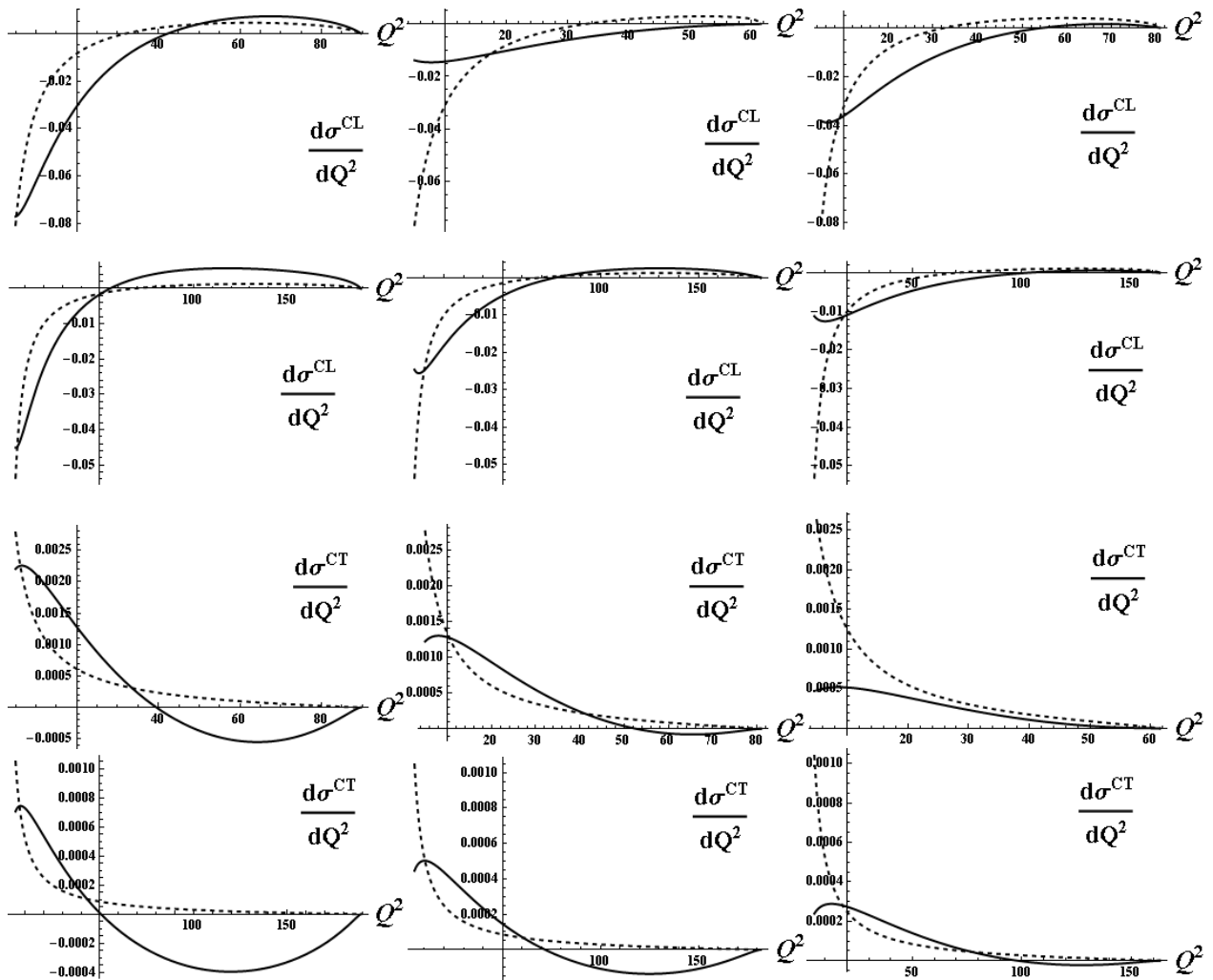

Fig 10. The same as in Fig. 9 but for the parts of the cross section which depend on the circular polarization of the photon. The first and second rows correspond to the longitudinal polarization of the target electron, the third and fourth rows – to the transversal one.
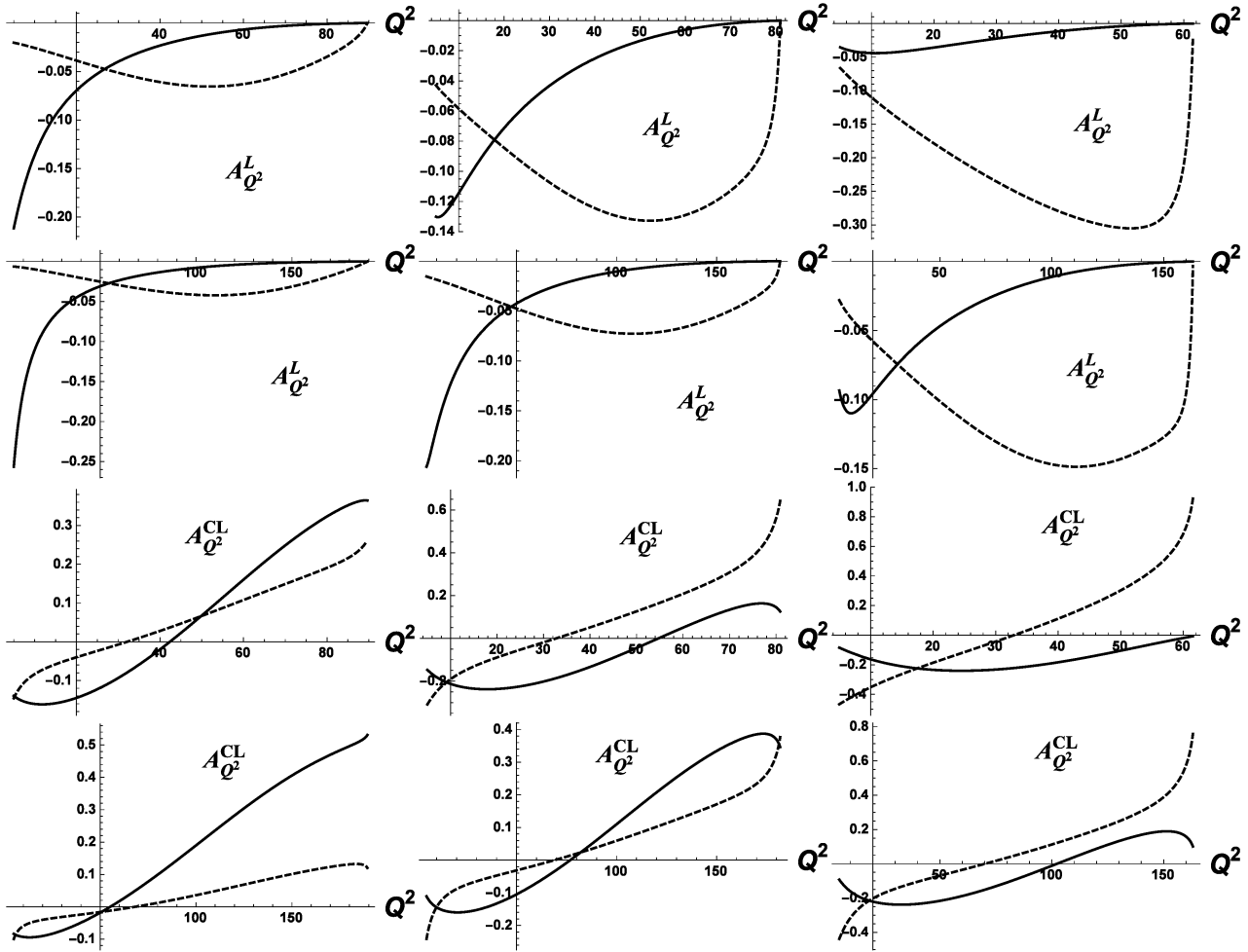
Fig 11. The L — and CL —asymmetries as functions of the created e^+e^- -pair invariant mass squared Q^2 at $\omega = 100$ MeV (the first and third rows) and $\omega = 200$ MeV (the second and fourth rows). The left (middle, right) panels correspond to the events with $q_m^2 < 10$ (20, 40) MeV^2. The dashed (solid) lines describe the ($\gamma - e^-$) (Borsellino) contribution.

CONCLUSION

In this paper, we analyzed the process of the triplet photoproduction on a polarized electron target by a polarized photon beam. The calculation of various observables has been done in the approach when four Feynman diagrams were taken into account. Besides the two Borsellino diagrams we took into account the two ($\gamma - e^-$) (or Compton-like) diagrams. So, we neglect the effects of the final electron identity. The results obtained in a such approximation describe the events with well separated created and recoil electrons. Otherwise, it is necessary to take into account the identity effects. The numerical calculations were performed in the laboratory system for the photon energy less than 200 MeV.

We investigated the possibility of determining the circular polarization degree of a high energy photon by measuring the asymmetry in the triplet production by a circularly polarized photon beam on a polarized electron target. The influence of the ($\gamma - e^-$) diagrams contribution on the calculated observables are also analysed.

We think that the measuring the distribution over the invariant mass of the created electron-positron pair in the process of the triplet photoproduction would be a good method to search for a dark photon. So, we search for the kinematical regions where the contribution of the dominated background mechanism (the Borsellino diagrams) can be suppressed as compared with the useful Compton-like diagrams where the signal from the dark photon may be measured. Besides, the contribution of the Borsellino diagrams can be calculated with the necessary accuracy.

For the first time, the different distributions were obtained in the analytical form. We obtain the double distribution over the q^2 (the square of the four-momentum transfer to the recoil electron) and Q^2 (the created e^+e^- -pair invariant mass squared) variables, and single distributions over the q^2 or Q^2 variables.

We obtain the expressions for the asymmetry A^L caused by the linear polarization of the photon beam as a function of the photon energy ω and as a function of q_m^2 at fixed ω. The asymmetries A^{CL} (A^{CT}), caused by the circularly polarized photon beam and polarized initial electron in the case when the polarization vector of the target is parallel (orthogonal) to the photon momentum, have been also calculated as a functions of q_m^2 and ω. Although the

final expressions for all the observables are given in the laboratory system but until this step all the expressions are given in the invariant form and it is easy to transform the final expressions to the invariant form by the substitution $\omega = (W^2 - 2m^2)/2m$. It was found that the measurement of the A^{CL} or $A^{CL}_{q^2_m}$ asymmetries can be used for the determination of the circular polarization of the photon beam for the $\omega \leq 20\,(200)$ MeV for the case of A^{CL} $(A^{CL}_{q^2_m})$.

Acknowledgments

REFERENCES

1. Haug. E. Bremsstrahlung and Pair Production in the Field of Free Electrons // Z. Naturforsch. – 1975. – Vol. 30a. – P.1099-1113.
2. Borsellino A. Sulle coppie di elettroni create da raggi in prezenza di elettroni // Nuovo. Cim. – 1947. – Vol.4. – P.112-130.
3. Mork K.J. Pair Production by Photons on Electrons // Phys. Rev. – 1967. – Vol.160. – P.1065-1071.
4. Haug. E. Simple Analytic Expressions for the Total Cross Section for $\gamma-e$ Pair Production // Z. Naturforsch. – 1981. – Vol. 36a. – P.413 -414.
5. Endo I., Kobayashi T. Exact evaluation of triplet photoproduction // Nucl. Instr. and Meth. – 1993. – Vol.A328. – P.517-521.
6. Ahmadov A.I., Galynskii M.V., Bystritskiy Yu.M. et al. QED peripheral mechanism of pair production at colliders // Phys. Rev. – 2008. – Vol.D78. – 074015.
7. Iparraguirre M.L., Depaola G.O. About Electrons in Triplet Production // arXiv; 1406.3001 v1. – 2014. – [hep-ph].
8. Baier V.N., Fadin V.S. Khoze V.A. Electromagnetic pair production // Zh. Eksp. Teor. Fiz. – 1966. – Vol.50. – P.156-168.
9. Boldyshev V.F., Peresun'ko Yu.P. Electron-positron pair production on electrons and analysis of photon beam polarization // Yad. Fiz. – 1971. – Vol.14. – P.1027-1032.
10. Boldyshev V.F., Peresun'ko Yu.P. On determination of photon polarization from asymmetry of the recoil electrons in triplets // Yad. Fiz. – 1974. – Vol.19. – P.144-147.
11. Vinokurov E.A., Kuraev E.A. Production of Triplets by Polarized Photons // Zh. Eksp. Teor. Fiz. – 1973. – Vol.63. – P.1142-1150.
12. Vinokurov E.A., Merenkov. N.P. On Production of Triplets by High-Energy Polarized Photons // Yad. Fiz. – 1975. – Vol.21. – P.781-784.
13. Boldyshev V.F., Vinokurov E.A., Peresun'ko Yu.P., Merenkov N.P. A Method for Measurement of the Photon Beam Linear Polarization by Means of Recoil Electron Asymmetry in the e^+e^- -Pair Photoproduction on Electrons // Physics of Elementary Particles and Atomic Nuclei – 1994. – Vol.25. – P.696-778.
14. Akushevich I.V. et al. Triplet production by linearly polarized photons // Phys. Rev. – 2000. – Vol.A61. – 032703.
15. Gakh G.I., Konchatnij M.I., Levandovsky I.S., Merenkov N.P. Analysis of Triplet Production by a Circularly Polarized Photon at High Energies // Zh. Eksp. Teor. Fiz. – 2013. – Vol.144. – P60-74.
16. Endo I. et al. Detection of recoil electrons in triplet photoproduction // Nucl. Instr. and Meth.-1989. – Vol.A280. – P.144-146.
17. Depaola G.O., Iparraguirre M.L. Angular distribution for the electron recoil in pair production by linearly polarized γ -rays on electrons // Nucl. Instr. and Meth. – 2009. – Vol.A611. – P.84-92.
18. Pak A.V., Pavluchenko D.V., Petrosyan S.S., et al. Measurement of $\gamma\gamma$ and γe luminosities and polarizations at photon colliders // Nucl. Phys. (Proc. Suppl.). – 2004. – Vol.B126. – P.379-385.
19. IRIDE. Interdisciplinary Research Infrastructure based on Dual Electron linac and lasers // Nucl. Instr. and Meth.-2014. – Vol.A740. – P.138-146; Alesini D. et al. IRIDE White Book, An Interdisciplinary Research Infrastructure based on Dual Electron linac &lasers // arXiv:1307.7967v1 [physics.ins-det], 270 PP.
20. Fayet P. U-boson production in e^+e^- annihilation, Ψ and Y decays - Phys. Rev. – 2007. – Vol.D75. – 115017; Arkani-Hamed N. et al. A theory of dark matter // Phys. Rev. – 2009. – Vol.D79. – 015014; Pospelov M. Secluded U(1) below the weak scale // Phys. Rev. – 2009. – Vol.D80. – 095002.
21. Pauk Vladislav and Vanderhaegen Marc. Lepton Universality Test in the Photoproduction of e^+e^- versus $\mu^+\mu^-$ Pairs on a Proton Target // Phys. Rev. Lett. – 2015. – Vol.115. – 221804.
22. Byrd Paul F., Friedman Morris D. Handbook of Elliptic Integrals for Engineers and Sientists, Second Edition, Springer-Verlag New York Heidelberg Berlin, 1971.
23. HADES Collaboration. Searching a Dark Photon with HADES // Phys. Lett. -.2014. – Vol.B731.- P.265-271.
24. Lees J.P. et al. Search for a Dark Photon in e^+e^- - Collisions at BaBar // Phys. Rev. Lett. – 2014. – Vol.113. – 201801.
25. Batell B. Strong Constraints on Sub-GeV Dark Sector from SLAC Beam Dump E137 // Phys. Rev. Lett. – 2014. – Vol.113. – 171802.
26. Andreas S. Hidden Photons in beam dump experiments and in connection with Dark Matter // Frascati Phys. Ser. – 2012. – Vol.56. – P. 23-32.
27. Izaguirre E. et al. Physics motivation for a pilot dark matter search at Jefferson Laboratory // Phys. Rev. – 2014. – Vol.D90. – 014052.
28. Soffer A. Search for Light Scalars, Pseudoscalars, and Gauge Bosons // arXiv: 1507.0233v1. – 2015. – [hep-ex].
29. Berestetskii V.B., Lifshitz E.M., Pitaevskii. Quantum Electrodynamics, Moscow: Nauka, 1989; Oxford: Pergamon, 1994. – P.221.
30. Mork K., Olsen H. Radiative Corrections. I. High-Energy Bremsstrahlung and Pair Production // Phys. Rev. – 1965. – Vol.B140. – P.1661-1674; Vinokurov E.A., Kuraev E.A., Merenkov N.P. Radiative corrections to e^+e^- pair production by a high-energy photon in the field of an electron or a nucleus // Zh. Eksp. Teor. Fiz. – 1974. – Vol.66. – P.1916-1925